arXiv:1302.0672v1 [hep-ph] 4 Feb 2013

Preprint typeset in JHEP style - HYPER VERSION

Neutrino masses, dominant neutrinoless double beta decay, and observable lepton flavor violation in left-right models and SO(10) grand unification with low mass $\mathrm{W_R}, \mathrm{Z_R}$ bosons

---

Ram Lal Awasthi,[δ] **M. K. Parida**[†] **and Sudhanwa Patra**[†]

[†]*Center of Excellence in Theoretical and Mathematical Sciences, Siksha 'O' Anusandhan University, Bhubaneswar-751030, India*
[δ]*Harish-Chandra Research Institute, Chhatnag Road, Jhusi, Allahabad 211019, India,*

E-mails: `ramlal@hri.res.in`, `paridamk@soauniversity.ac.in`,
`sudha.astro@gmail.com`

Abstract: While the detection of W_R-boson at the Large Hadron Collider is likely to resolve the mystery of parity violation in weak interaction, observation of neutrinoless double beta decay rate is expected to determine whether neutrinos are Majorana fermions. In the conventional TeV scale parity restoring left-right model, new dominant contribution to neutrinoless double beta decay runs into conflict with light neutrino mass predictions through popular seesaw mechanisms. We evade this difficulty by using a class of left-right gauge theories with high scale parity restoration but TeV scale W_R, Z_R gauge bosons and extended seesaw mechanism for neutrino masses. Most dominant new contribution to neutrinoless double beta decay is noted to occur via $W_L^- W_L^-$ mediation involving lighter sterile neutrino exchanges. The next dominant contribution is found to be through $W_L^- W_R^-$ mediation involving both light and heavy right-handed neutrino or sterile neutrino exchanges. The quark-lepton symmetric origin of the Dirac neutrino mass matrix is also found to play a crucial role in determining these results while predicting lepton flavor violating branching ratios for $\tau \to e + \gamma$, $\tau \to \mu + \gamma$, and $\mu \to e + \gamma$ accessible to ongoing search experiments. The underlying non-unitarity matrix is found to manifest in the predictions of substantial CP-violating effects even when the leptonic Dirac phase $\delta_{\mathrm{CP}} \simeq 0, \pi, 2\pi$. Finally we explore a possible origin of the model in non-supersymmetric SO(10) grand unified theory where, in addition to low mass $W_R^{\pm}$ and Z_R bosons accessible to Large Hadron Collider, the model is found to predict observable neutron-antineutron oscillation and lepto-quark gauge boson mediated rare kaon decay with $\mathrm{Br}\,(K_{\mathrm{L}} \to \mu\, \bar{e}) \simeq \left(10^{-9} - 10^{-11}\right)$.

Keywords: Beyond Standard Model, neutrino masses and mixing, neutrinoless double beta decay, Lepton Flavor Violation, Grand Unified Theory.

Contents

1. Introduction **2**

2. Low scale left-right gauge theory and extended seesaw mechanism **3**
- 2.1 The model 3
- 2.2 Neutrino masses and mixings 4
- 2.3 The unitarity violating matrix 5
- 2.4 Determination of μ_S from fits to neutrino oscillation data 8

3. Amplitudes for $0\nu\beta\beta$ decay and effective mass parameters **9**
- 3.1 $W_L^- - W_L^-$ mediation 9
- 3.2 $W_R^- - W_R^-$ mediation 10
- 3.3 $W_L^- - W_R^-$ mediation 11
- 3.4 Doubly Charged Higgs contribution 11
- 3.5 Effective mass parameters 12

4. Numerical estimation of effective mass parameters **12**
- 4.1 Nearly standard contribution 13
- 4.2 Dominant non-standard contributions 13

5. Predictions on lepton flavor violating decays and $\mathbf{J}_{\mathrm{CP}}$ **16**
- 5.1 Branching ratio 16
- 5.2 CP-violation due to non-unitarity 18

6. Implementation in SO(10) **19**
- 6.1 Symmetry breaking chain 19
- 6.2 Gauge coupling unification 20
- 6.3 Physical significance of mass scales 21
- 6.4 Importance of $\mathcal{G}_{224D}$ intermediate symmetry 22
- 6.5 Prediction of Dirac neutrino mass matrix 22

7. Summary and Conclusion **22**

A. APPENDIX **23**
- A.1 Block diagonalization and determination of $\mathcal{M}_{\mathrm{BD}}$ 24
  - A.1.1 Determination of $\mathcal{W}_1$ 24
  - A.1.2 Determination of $\mathcal{W}_2$ 25
- A.2 Complete diagonalization and physical neutrino masses 26

B. One- and two-loop beta function coefficients for RG evolution of gauge couplings **27**

1. Introduction

The Standard Model (SM) of strong, weak, and electromagnetic interactions has successfully confronted numerous experimental tests, yet its failures are exposed in neutrino masses and mixings, dark matter, dark energy, and baryon asymmetry of the universe. Apart from containing a number of unknown parameters, the model does not explain why parity violation is monopoly of weak interaction. The suggestion of the origin of parity restoration is almost as old as the suggestion of parity violation itself when Lee and Yang [1] conjectured all basic interactions to be left-right symmetric. Subsequently, two classes of theories have been proposed to achieve the desired goal: (**a**) mirror symmetric extension of the Standard Model [2], (**b**) proposal of left-right symmetric gauge theory based upon $SU(2)_L \times SU(2)_R \times SU(4)_C$ ($\equiv \mathcal{G}_{224D}$) [3] and $SU(2)_L \times SU(2)_R \times U(1)_{B-L} \times SU(3)_C$ ($\equiv \mathcal{G}_{2213D}$) [4] with $g_{2L} = g_{2R}$. The minimal rank 5 grand unified theory (GUT) like SO(10) [5] contains G_{224D} and G_{2213D} as its subgroups. The canonical ($\equiv$ type-I) and type-II seesaw mechanisms [6–9] explaining tiny left-handed (LH) neutrino masses emerge naturally from SO(10), G_{224D}, and G_{2213D} gauge theories provided both left-handed (LH) and right-handed (RH) neutrinos are Majorana fermions

$$m_\nu^I = -M_D \frac{1}{M_N} M_D^T \,, \qquad\qquad m_\nu^{II} = f\, v_L \,, \tag{1.1}$$

where m_ν^I (m_ν^{II}) is the type-I (type-II) prediction of light LH neutrino mass matrix, M_D (M_N) is the Dirac (right-handed Majorana) neutrino mass, and $v_L = \lambda v_{WK}^2 / M_{\Delta_L}$, v_{WK} and M_{Δ_L} being the electroweak vacuum expectation value (VEV), and left-handed triplet mass, respectively. Here f (λ) is the associated Majorana (Higgs-quartic) coupling. Currently a number of dedicated experiments on neutrinoless double beta ($0\nu\beta\beta$) decay are in progress [10] while Heidelberg-Moscow experiment [11] has already claimed to have measured the effective mass parameter $M_{ee}^{\rm eff} \simeq (0.23 - 0.56)$ eV and this observation might be hinting towards the Majorana nature of the light neutrinos [12].

SO(10) GUT has the advantage of unifying the three basic forces (excluding gravity) and all fermions of the SM plus the RH neutrinos are unified into a single spinorial representation **16** of $SO(10)$. In view of the underlying quark-lepton symmetry $\mathcal{G}_{224D}$ [3] of $SO(10)$, the Dirac neutrino mass matrix M_D is similar to the up-quark mass matrix M_u in these theories, although $\mathcal{G}_{2213D}$ [4] has also the alternative possibility of M_D to be similar to the charged lepton mass matrix M_ℓ if the symmetry does not emerge from $\mathcal{G}_{224D}$ or $SO(10)$. In any case, tiny neutrino masses uncovered by the neutrino oscillation experiments [13] push the seesaw scales to be $> 10^{10}$ GeV rendering both the seesaw mechanisms to be inaccessible for direct experimental tests. In the process, the large scale of the associated RH gauge bosons ($W_R^\pm$, Z_R) prevent any visible nonstandard impact on weak interaction phenomenology including $0\nu\beta\beta$ decay [9] while throwing out the origin of left-right symmetric theory out of the arena of direct experimental tests at Large Hadron Collider (LHC) and other high energy accelerators in foreseeable future. This has led to alternative ways within conventional LR gauge theories with sub dominant Dirac neutrino masses so that light neutrino masses and nonstandard $0\nu\beta\beta$ decay rates are predicted with TeV scale $W_R^\pm$ and Z_R boson masses accessible to LHC and future accelerators [14–16].

In this work we adopt the view that the Dirac neutrino masses are natural predictions of left-right gauge theories because of their high scale origins from $\mathcal{G}_{224D}$ or $SO(10)$. We show how a different class of left-right models [17] having the property of high scale parity restoration but with minimal extension to accommodate experimentally testable extended seesaw mechanism [18, 19] predicts the light neutrino masses to be governed by gauged inverse seesaw formula while giving dominant contributions to $0\nu\beta\beta$ decay. The masses of $W_R^{\pm}$ and Z_R gauge bosons, and RH neutrinos could be of $\mathcal{O}(\text{TeV})$ [20] which are also directly accessible to accelerator tests [21]. The model predicts quite dominant contributions to $0\nu\beta\beta$ decay rate through two specific Feynman diagrams, one with $W_L^- - W_L^-$ mediation and relatively light sterile neutrino exchanges, and the other via $W_L^- - W_R^-$ mediation with exchanges of light LH and heavy RH neutrinos or sterile neutrinos. The model also predicts substantial non-unitarity effects and lepton flavor violating (LFV) decays accessible to ongoing experimental searches for $\tau \to e + \gamma$, $\tau \to \mu + \gamma$, and $\mu \to e + \gamma$. Finally we show how such a TeV scale LR gauge theory emerges from a non-supersymmetric (non-SUSY) SO(10) grand unification framework. The grand unified theory also predicts experimentally observable neutron-antineutron oscillation [22] and rare kaon decay $\text{Br}\left(K_L \to \mu\,\overline{e}\right) \simeq \left(10^{-9} - 10^{-11}\right)$ [23] mediated by lepto-quark gauge boson of $SU(4)_C$, although proton lifetime is found to be beyond the accessible limit of ongoing experiments.

The plan of this paper is organized as follows: in Sec. **2** we briefly discuss the TeV scale left-right gauge theory with low-mass W_R, Z_R bosons, light neutrino masses and associated non-unitarity effects; in Sec **3**, we present the various Feynman amplitudes to neutrinoless double beta decay; in Sec **4**, we give a detailed discussion for standard and non-standard contributions to the effective mass parameter for $0\nu2\beta$ decay rate; in Sec **5**, we have discussed the branching ratios for lepton flavor violating decays; in Sec **6**, we implement the idea in a SO(10) grand unified theory, and in Sec **7** we summarize and conclude our results.

2. Low scale left-right gauge theory and extended seesaw mechanism

2.1 The model

As in the case of extended seesaw mechanism in LR models [19,24], besides the standard 16-fermions of each generation, we add one additional sterile fermion singlet for each generation ($S_i, i = 1, 2, 3$). We start with parity conserving left-right symmetric gauge theory, $\mathcal{G}_{224D}$ [3] or $\mathcal{G}_{2213D}$ [4], with equal gauge couplings ($g_{2L} = g_{2R}$) at high scales. In the Higgs sector we need both LH and RH triplets ($\mathbf{\Delta_L}, \mathbf{\Delta_R}$) as well as the LH and RH doublets ($\chi_\mathbf{L}, \chi_\mathbf{R}$) in addition to the bidoublet ($\mathbf{\Phi}$) and a D-parity odd singlet σ [17]. Their transformation properties under $\mathcal{G}_{224D} \supset \mathcal{G}_{2213D}$ are

$$\begin{aligned}
\Delta_L(3,1,10) \supset \Delta_L(3,1,-2,10), &\quad \Delta_R(1,3,\overline{10}) \supset \Delta_L(3,1,-2,1), \\
\Phi(2,2,1) \supset \Phi(2,2,0,1), &\quad \chi_L(1,2,4) \supset \chi_L(1,2,-1,1), \\
\chi_R(2,1,\overline{4}) \supset \chi_R(2,1,-1,1), &\quad \sigma(1,1,1) \supset \sigma(1,1,0,1).
\end{aligned} \tag{2.1}$$

When the D-parity odd singlet σ acquires a VEV $\langle\sigma\rangle \sim M_P$ the LR symmetry is spontaneously broken leading to $M^2_{\Delta_R} = (M^2_\Delta - \lambda_\Delta \langle\sigma\rangle M')\Delta^\dagger_R \Delta_R$, $M^2_{\chi_R} = (M^2_\chi - \lambda_\chi \langle\sigma\rangle M')\chi^\dagger_R \chi_R$, where $\lambda_\Delta, \lambda_\chi$ are trilinear couplings and $\langle\sigma\rangle$, M', M_Δ, M_χ are all $\sim \mathcal{O}(M_P)$, the RH Higgs scalar masses are made lighter depending upon the degree of fine tuning in λ_Δ and λ_χ. The asymmetry in the Higgs sector causes asymmetry in the $SU(2)_L$ and $SU(2)_R$ gauge couplings with $g_{2L}(\mu) > g_{2R}(\mu)$ for $\mu < M_P$. We then break $G_{2213} \to$ SM by the VEV of the right handed triplet $\langle\Delta^0_R\rangle \sim v_R$ whereas the VEV of the RH-doublet $\langle\chi^0_R\rangle = v_\chi$ provides the $N - S$ mixing. The G_{2213} symmetric low-scale Yukawa Lagrangian is

$$\begin{aligned}\mathcal{L}_{\rm Yuk} &= Y^\ell \overline{\psi}_L\, \psi_R\, \Phi + f\, \psi^c_R\, \psi_R \Delta_R + F\, \overline{\psi}_R\, S\, \chi_R \\ &+ S^T \mu_S S + \text{h.c.}\end{aligned} \tag{2.2}$$

which gives rise to the 9×9 neutral fermion mass matrix after the electroweak symmetry breaking

$$\mathcal{M} = \begin{pmatrix} 0 & 0 & M_D \\ 0 & \mu_S & M \\ M_D^T & M^T & M_N \end{pmatrix}, \tag{2.3}$$

where $M_D = Y\langle\Phi\rangle$, $M_N = f\langle\Delta^0_R$, $M = F\langle\chi^0_R\rangle$. Here M_D and M are general complex matrices while M_N and μ_S are complex symmetric matrices.

2.2 Neutrino masses and mixings

In this model the RH neutrinos being heavier than the other mass scales with $M_N \gg M > M_D, \mu_S$ are at first integrated out from the Lagrangian leading to [18]

$$\begin{aligned}-\mathcal{L}_{\rm eff} = \left(M_D \frac{1}{M_N} M_D^T\right)_{\alpha\beta} \nu^T_\alpha \nu_\beta + \left(M_D \frac{1}{M_N} M^T\right)_{\alpha m} \left(\overline{\nu_\alpha} S_m + \overline{S_m} \nu_\alpha\right) \\ + \left(M \frac{1}{M_N} M^T\right)_{mn} S^T_m S_n - \mu_S S^T_m S_n\,,\end{aligned} \tag{2.4}$$

which, in the $(\nu,\ S)$ basis, gives the 6×6 mass matrix

$$\mathcal{M}_{\rm eff} = -\begin{pmatrix} M_D M_N^{-1} M_D^T & M_D M_N^{-1} M^T \\ M M_N^{-1} M_D^T & M M_N^{-1} M^T - \mu_S \end{pmatrix}, \tag{2.5}$$

while the 3×3 heavy RH neutrino mass matrix M_N is the other part of the full 9×9 neutrino mass matrix. This 9×9 mass matrix $\tilde{\mathcal{M}}_{\rm BD}$ which results from the first step of block diagonalization procedure as discussed above and in the appendix is

$$\mathcal{W}_1^\dagger \mathcal{M}_\nu \mathcal{W}_1^* = \tilde{\mathcal{M}}_{\rm BD} = \begin{pmatrix} \mathcal{M}_{\rm eff} & 0 \\ 0 & M_N \end{pmatrix}, \tag{2.6}$$

where $\mathcal{W}_1$ has been derived as shown in eqn. (A.10) of the appendix.

After the second step of block diagonalization, the type-I seesaw contribution cancels out and gives in the (ν, S, N) basis

$$\mathcal{W}_2^\dagger \tilde{\mathcal{M}}_{\rm BD} \mathcal{W}_2^* = \mathcal{M}_{\rm BD} = \begin{pmatrix} m_\nu & 0 & 0 \\ 0 & m_{\mathcal{S}} & 0 \\ 0 & 0 & m_{\mathcal{N}} \end{pmatrix} , \tag{2.7}$$

where $\mathcal{W}_2$ has been derived in eqn. (A.20) of the appendix. In eqn. (2.7), the three 3×3 matrices are

$$m_\nu \sim M_D M^{-1} \mu_S (M_D M^{-1})^T \tag{2.8}$$
$$m_{\mathcal{S}} \sim \mu_S - M M_N^{-1} M^T \tag{2.9}$$
$$m_{\mathcal{N}} \sim M_N \, , \tag{2.10}$$

the first of these being the well known inverse seesaw formula [25, 26].

In the third step, m_ν, $m_{\mathcal{S}}$, and $m_{\mathcal{N}}$ are further diagonalized by the respective unitary matrices to give their corresponding eigenvalues

$$\begin{aligned} U_\nu^\dagger \, m_\nu \, U_\nu^* &= \hat{m}_\nu = \text{diag}\left(m_{\nu_1}, m_{\nu_2}, m_{\nu_3}\right) \, , \\ U_S^\dagger \, m_{\mathcal{S}} \, U_S^* &= \hat{m}_S = \text{diag}\left(m_{S_1}, m_{S_2}, m_{S_3}\right) \, , \\ U_N^\dagger \, m_{\mathcal{N}} \, U_N^* &= \hat{m}_N = \text{diag}\left(m_{N_1}, m_{N_2}, m_{N_3}\right) \, . \end{aligned} \tag{2.11}$$

The complete mixing matrix [24, 27] diagonalizing the above 9×9 neutrino mass matrix given in (2.3) turns out to be

$$\mathcal{V} \equiv \begin{pmatrix} \mathcal{V}^{\nu\hat{\nu}}_{\alpha i} & \mathcal{V}^{\nu\hat{S}}_{\alpha j} & \mathcal{V}^{\nu\hat{N}}_{\alpha k} \\ \mathcal{V}^{S\hat{\nu}}_{\beta i} & \mathcal{V}^{S\hat{S}}_{\beta j} & \mathcal{V}^{S\hat{N}}_{\beta k} \\ \mathcal{V}^{N\hat{\nu}}_{\gamma i} & \mathcal{V}^{N\hat{S}}_{\gamma j} & \mathcal{V}^{N\hat{N}}_{\gamma k} \end{pmatrix} \tag{2.12}$$

$$= \begin{pmatrix} \left(1 - \frac{1}{2} X X^\dagger\right) U_\nu & \left(X - \frac{1}{2} Z Y^\dagger\right) U_S & Z \, U_N \\ -X^\dagger \, U_\nu & \left(1 - \frac{1}{2}\{X^\dagger X + Y Y^\dagger\}\right) U_S & \left(Y - \frac{1}{2} X^\dagger Z\right) U_N \\ y^* \, X^\dagger \, U_\nu & -Y^\dagger \, U_S & \left(1 - \frac{1}{2} Y^\dagger Y\right) \, U_N \end{pmatrix} , \tag{2.13}$$

as shown in the appendix. In eqn. (2.13) $X = M_D \, M^{-1}$, $Y = M \, M_N^{-1}$, $Z = M_D \, M_N^{-1}$, and $y = M^{-1} \, \mu_S$.

2.3 The unitarity violating matrix

In this subsection our strategy is to first find M_D, M_N, M and μ_S using the inverse see-saw formula, neutrino oscillation data, up-quark masses and the CKM matrix elements. We consider the situation where the Dirac neutrino mass matrix is fixed by the underlying quark-lepton symmetry. Neglecting renormalization group (RG) corrections, it is taken to be approximately equal to the up-quark mass matrix [24]. Using CKM matrix elements, its Dirac phase, and the running masses of the three up-type quarks, namely, $m_u \simeq 2.33$

MeV, $m_c \simeq 1.275$ GeV and $m_t \simeq 160$ GeV [28], the Dirac neutrino mass matrix at the TeV scale is found to be [24, 29]

$$\begin{aligned} M_D \simeq M_u &= V_{\rm CKM} \hat{M}_u V_{\rm CKM}^T \\ &= \begin{pmatrix} 0.067 + 0.004i & 0.302 - 0.022i & 0.550 - 0.53i \\ 0.302 - 0.022i & 1.48 - 0.0i & 6.534 - 0.0009i \\ 0.55 - 0.53i & 6.534 - 0.0009i & 159.72 + 0.0i \end{pmatrix} \end{aligned} \tag{2.14}$$

As the predicted $0\nu\beta\beta$ decay rate is quite sensitive to M_D, we have also utilized it's value obtained including RG corrections where $M_D \simeq M_u$ holds at the GUT scale $M_{\rm GUT} \simeq 2 \times 10^{16}$ GeV) [30–32]

$$M_D = \begin{pmatrix} 0.0151 & 0.0674 - 0.0113i & 0.1030 - 0.2718i \\ 0.0674 + 0.0113i & 0.4758 & 3.4410 + 0.0002i \\ 0.1030 + 0.2718i & 3.4410 - 0.0002i & 83.450 \end{pmatrix} \text{GeV} \tag{2.15}$$

while most of our results will utilize eq. (2.15), we will also discuss the results obtained using eq. (2.14) in Sec. **4**.

Usually, diagonalizing the light active Majorana neutrino mass matrix by the PMNS mixing matrix $U_{\rm PMNS}$ gives, $U_{\rm PMNS}^\dagger \, m_\nu \, U_{\rm PMNS}^* = \hat{m}_\nu = \text{diag}\,(m_{\nu_1}, m_{\nu_2}, m_{\nu_3})$. But, in this extended seesaw scheme, diagonalization is done by a matrix $\mathcal{N} \equiv \mathcal{V}^{\nu\nu}$ which is a part of the full 9×9 mixing matrix $\mathcal{V}_{9\times 9}$. Using $\eta = \frac{1}{2} X X^\dagger$ where $X = M_D/M$, this diagonalizing matrix is

$$\mathcal{N} \simeq (1 - \eta) U_{\rm PMNS}. \tag{2.16}$$

Thus η is a measure of deviation from unitarity in the lepton sector on which there has been extensive investigations in different models [24,30,31,33,34]. Assuming M to be diagonal for the sake of simplicity, $M \equiv \text{diag}(M_1, M_2, M_3)$, gives $\eta_{\alpha\beta} = \frac{1}{2} \sum_k \, M_{D\alpha k} M_k^{-2} M_{D\beta k}^*$,

measure of non-unitarity	Expt. bound [33] **C0**	**C1**	**C2**	**C3**
$\lvert\eta_{ee}\rvert$	2.0×10^{-3}	3.4×10^{-8}	2.7×10^{-7}	2.7×10^{-6}
$\lvert\eta_{e\mu}\rvert$	3.5×10^{-5}	3.9×10^{-7}	1.8×10^{-6}	1.4×10^{-5}
$\lvert\eta_{e\tau}\rvert$	8.0×10^{-3}	9.4×10^{-6}	1.7×10^{-5}	6.1×10^{-5}
$\lvert\eta_{\mu\mu}\rvert$	8.0×10^{-4}	8.0×10^{-6}	1.5×10^{-5}	6.8×10^{-5}
$\lvert\eta_{\mu\tau}\rvert$	5.1×10^{-3}	1.1×10^{-4}	1.7×10^{-4}	3.2×10^{-4}
$\lvert\eta_{\tau\tau}\rvert$	2.7×10^{-3}	2.7×10^{-3}	2.7×10^{-3}	2.7×10^{-3}

Table 1: Experimental bounds of the non-unitarity matrix elements $\lvert\eta_{\alpha\beta}\rvert$ (column **C0**) and their predicted values for degenerate (column **C1**), partially-degenerate (column **C2**), and non-degenerate (column **C3**) values of $M = \text{diag}\,(M_1, M_2, M_3)$ as described in cases (**a**), (**b**) and (**c**), respectively, in the text.

but it can be written explicitly for the degenerate case ($M_1 = M_2 = M_3 = M_d$)

$$\eta = \frac{1\ \mathrm{GeV}^2}{M_d^2(\mathrm{GeV}^2)} \begin{pmatrix} 0.0447 & 0.1937 - 0.4704i & 4.4140 - 11.360i \\ 0.1937 + 0.4704i & 6.036 & 144.40 - 0.0002i \\ 4.4140 + 11.360i & 144.40 + 0.0002i & 3488.0 \end{pmatrix} . \tag{2.17}$$

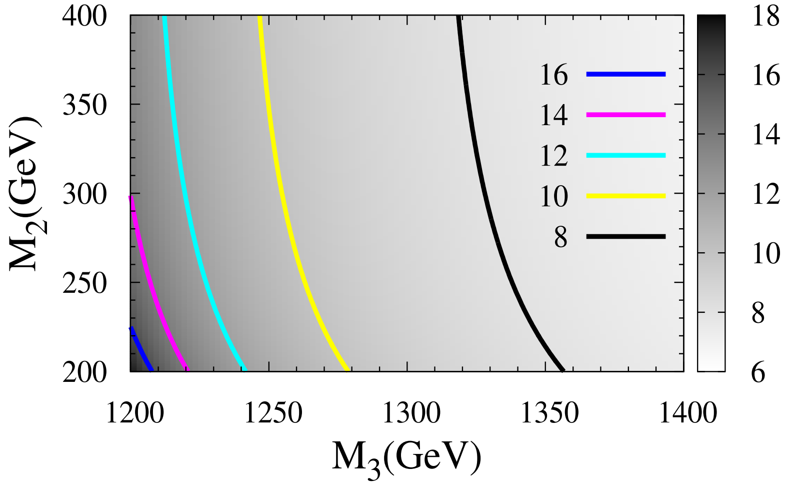

Figure 1: The contours of M_1 in the plane of M_2 and M_3. The solid curves in the diagram represent M_3 dependence of M_2 for fixed values of M_1 using eqn. (2.18). The brightest top-right corner suggests that lightest M_1 may exist for largest values of M_2 and M_3.

For the non degenerate diagonal matrix M, saturating the experimental bound for $|\eta_{\tau\tau}| < 2.7 \times 10^{-3}$ [24,31] gives

$$\frac{1}{2}\left[\frac{0.6640}{M_1^2} + \frac{48.8441}{M_2^2} + \frac{29138.9}{M_3^2}\right] = 2.7 \times 10^{-3} . \tag{2.18}$$

The correlation between M_2 and M_3 is shown in Fig. 1 where the allowed region in the brightest top right corner suggests the possibility of lightest M_1 for large values of M_2 and M_3. From eq. (2.18), Then the lightest possible mass is $M_1 = 3.96$ GeV in the limiting case $M_2, M_3 \to \infty$. Similarly lightest possible masses are $M_2 = 46.83$ GeV and $M_3 = 1135.61$ GeV in the other two limiting cases. When we assume equal contribution to nonunitarity from all three terms in the left hand side of eq.(2.18), we get perfectly reasonable condition for extreme non-degeneracy of $M = (6.85, 81.10, 1966.94)$ GeV. The elements of η have been listed in the Table. 1 for (**a**) degenerate $M = \mathrm{diag}(1136.6, 1136.6, 1136.6)$ GeV, (**b**) partially degenerate $M = \mathrm{diag}(100, 100, 1286.5)$ GeV, and (**c**) non degenerate $M = \mathrm{diag}(6.85, 81.1, 1966.9)$ GeV in columns **C1**, **C2** and **C3**, respectively, where in column **C0**, experimental bounds are presented [33].

m_ν	M	μ_S
NH	(a)	$\begin{pmatrix} 1.359 + 0.4106i & -0.2666 - 0.0822i & 0.0106 - 0.0016i \\ . & 0.0525 + 0.0164i & -0.0021 + 0.0003i \\ . & . & 0.00007 - 0.00003i \end{pmatrix}$ GeV
	(b)	$\begin{pmatrix} 0.0105 + 0.0032i & -0.0021 - 0.0006i & 0.0010 - 0.0002i \\ . & 0.0004 + 0.0001i & -0.0002 + 0.00003i \\ . & . & 0.00009 - 0.00006i \end{pmatrix}$ GeV
	(c)	$\begin{pmatrix} 0.494 + 0.149i & -1.147 - 0.353i & 1.104 - 0.163i \\ . & 2.675 + 0.835i & -2.582 + 0.367i \\ . & . & 2.022 - 1.339i \end{pmatrix} \times 10^{-4}$GeV

Table 2: Structure of μ_S from neutrino oscillation data for normal-hierarchy (NH) of light neutrino masses, $m_\nu = (0.00127, 0.008838, 0.04978)$ eV and different mass pattern of M: (**a**) $M = (1136.58, 1136.58, 1136.58)$ GeV, (**b**) $M = (100.0, 100.0, 1286.51)$ GeV, and (**c**) $M = (6.85, 81.10, 1966.94)$ GeV.

2.4 Determination of μ_S from fits to neutrino oscillation data

We utilize the central values of parameters obtained from recent global fit to the neutrino oscillation data [35]

$$\begin{aligned} &\sin^2\theta_{12} = 0.320, \quad \sin^2\theta_{23} = 0.427, \\ &\sin^2\theta_{13} = 0.0246, \;\; \delta_{CP} = 0.8\pi, \\ &\Delta m^2_{\rm sol} = 7.58 \times 10^{-5}{\rm eV}^2, \\ &|\Delta m_{\rm atm}|^2 = 2.35 \times 10^{-3}{\rm eV}^2, \end{aligned} \tag{2.19}$$

and ignore Majorana phases ($\alpha_1 = \alpha_2 = 0$). Then using the non-unitarity mixing matrix $\mathcal{N} = (1-\eta)\,U_{\rm PMNS}$ and the relation $m_\nu = \mathcal{N}\hat{m}_\nu\mathcal{N}^T$, we derive the μ_S matrix by inverting the inverse seesaw formula,

m_ν	M	μ_S
IH	(a)	$\begin{pmatrix} 14.6201 + 0.2741i & -2.7585 - 0.0603i & 0.0966 - 0.04549i \\ . & 0.5209 + 0.0130i & -0.0183 + 0.0085i \\ . & . & 0.0004 - 0.0006i \end{pmatrix}$ GeV
	(b)	$\begin{pmatrix} 0.1132 + 0.0021i & -0.0241 - 0.0005i & 0.0096 - 0.0045i \\ . & 0.0040 + 0.0001i & -0.0018 + 0.0008i \\ . & . & 0.0006 - 0.0008i \end{pmatrix}$ GeV
	(c)	$\begin{pmatrix} 0.5313 + 0.010i & -1.1866 - 0.0260i & 1.0078 - 0.4746i \\ . & 2.6524 + 0.0662i & -2.2567 + 1.0530i \\ . & . & 1.4561 - 1.8277i \end{pmatrix} \times 10^{-3}$GeV

Table 3: Same as Tab. 2 but for inverted-hierarchy (IH) of light neutrino masses $m_\nu = (0.04901, 0.04978, 0.00127)$ eV.

$$\begin{aligned}\mu_S &= X^{-1}\mathcal{N}\hat{m}_\nu\mathcal{N}^T\,(X^T)^{-1}\\ &= \begin{pmatrix} 0.494+0.149i & -1.147-0.353i & 1.104-0.163i\\ . & 2.675+0.835i & -2.582+0.367i\\ . & . & 2.022-1.339i \end{pmatrix}\times 10^{-4}\,\text{GeV}\end{aligned} \tag{2.20}$$

where we have used normal hierarchy (NH) for light neutrino masses, $\hat{m}_\nu = (0.00127, 0.00885, 0.0495)$ eV in the non degenerate case of $M = \text{diag}\,(16.85, 81.10, 1966.94)$ GeV. For the sake of completeness, we have presented few solutions of μ_S matrix for degenerate, partially-degenerate and non-degenerate values of M as shown in the Tables 2 and 3 corresponding to NH and IH light neutrino masses, respectively. For the quasi-degenerate (QD) pattern of light neutrino masses the matrix μ_S can be easily derived and all our analyses carried out in Sec. **3-5** can be repeated.

3. Amplitudes for $0\nu\beta\beta$ decay and effective mass parameters

In this section we discuss analytically the contributions of various Feynman diagrams in $W^-_L - W^-_L$, $W^-_R - W^-_R$, and $W^-_L - W^-_R$ channels and estimate the corresponding amplitudes in the TeV scale asymmetric left-right gauge theory with extended seesaw mechanism.

The charged current interaction Lagrangian for leptons in this model in the flavor basis is

$$\mathcal{L}_{\text{CC}} = \frac{g}{\sqrt{2}}\sum_{\alpha=e,\mu,\tau}\left[\overline{\ell}_{\alpha\,L}\,\gamma_\mu \nu_{\alpha\,L}\,W^\mu_L + \overline{\ell}_{\alpha\,R}\,\gamma_\mu N_{\alpha\,R}\,W^\mu_R\right] + \text{h.c.} \tag{3.1}$$

Following the masses and mixing for neutrinos in extended seesaw scheme [24] discussed in Sec. **2**, LH and RH neutrino flavor states are expressed in terms of mass eigenstates ($\hat{\nu}_i$, $\hat{S}_i$, $\hat{N}_i$)

$$\nu_{\alpha\,L} \sim \mathcal{V}^{\nu\nu}_{\alpha\,i}\,\hat{\nu}_i + \mathcal{V}^{\nu\,S}_{\alpha\,i}\,\hat{S}_i + \mathcal{V}^{\nu\,N}_{\alpha\,i}\,\hat{N}_i, \tag{3.2}$$

$$N^C_{\alpha\,R} \sim \mathcal{V}^{N\,\nu}_{\alpha\,i}\,\hat{\nu}_i + \mathcal{V}^{N\,S}_{\alpha\,i}\,\hat{S}_i + \mathcal{V}^{NN}_{\alpha\,i}\,\hat{N}_i. \tag{3.3}$$

As it is evident from the charged-current interaction given in eqn. (3.1), there can be several Feynman diagrams which contribute to neutrinoless double beta decay transition in the TeV scale left-right gauge theory. They can be broadly classified as due to $W^-_L - W^-_L$, $W^-_R - W^-_R$, and $W^-_L - W^-_R$ mediations which are denoted by LL, RR, and LR in the superscripts of the corresponding amplitudes. These diagrams are shown in Fig. 2, Fig. 3, and Fig. 4.

3.1 $W^-_L - W^-_L$ mediation

The most popular standard contribution is due to $W^-_L - W^-_L$ mediation by light neutrino exchanges. But one of our major contribution in this work is that even with $W^-_L - W^-_L$ mediation, the sterile neutrino exchange allowed within the extended seesaw mechanism of the model can yield much more dominant contribution to $0\nu\beta\beta$ decay rate than the

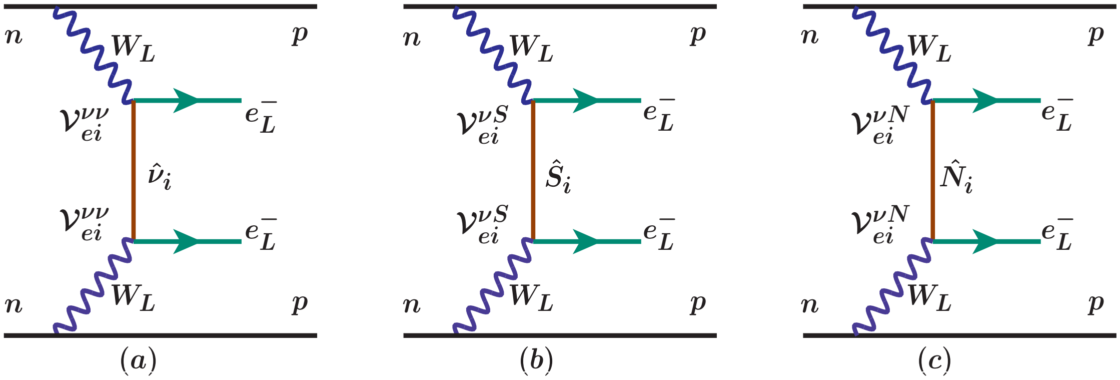
n
p
W_L
$\mathcal{V}^{\nu\nu}_{ei}$
e^-_L
$\hat{\nu}_i$
$\mathcal{V}^{\nu\nu}_{ei}$
e^-_L
W_L
n
p
(a)
$\mathcal{V}^{\nu S}_{ei}$
$\hat{S}_i$
$\mathcal{V}^{\nu S}_{ei}$
(b)
$\mathcal{V}^{\nu N}_{ei}$
$\hat{N}_i$
$\mathcal{V}^{\nu N}_{ei}$
(c)

Figure 2: Feynman diagrams for neutrinoless double beta decay ($0\,\nu\,\beta\beta$) contribution with virtual Majorana neutrinos $\hat{\nu}_i$, $\hat{S}_i$, and $\hat{N}_i$ along with the mediation of two W_L-bosons.

standard one. With the exchange of left-handed light neutrinos ($\hat{\nu}_i$), sterile neutrinos ($\hat{S}_j$), and RH heavy Majorana neutrinos ($\hat{N}_k$), the diagrams shown in Fig. 2.(a), Fig. 2.(b), and Fig. 2.(c) contribute

$$\mathcal{A}_\nu^{LL} \propto \frac{1}{M_{W_L}^4}\frac{\left(\mathcal{V}_{e\,i}^{\nu\nu}\right)^2\, m_{\nu_i}}{p^2}\,, \tag{3.4}$$

$$\mathcal{A}_S^{LL} \propto \frac{1}{M_{W_L}^4}\frac{\left(\mathcal{V}_{e\,j}^{\nu S}\right)^2}{m_{S_j}}\,, \tag{3.5}$$

$$\mathcal{A}_N^{LL} \propto \frac{1}{M_{W_L}^4}\frac{\left(\mathcal{V}_{e\,k}^{\nu N}\right)^2}{m_{N_k}}\,, \tag{3.6}$$

where $|p^2| \simeq (190\text{ MeV})^2$ represents neutrino virtuality momentum [36].

3.2 $W_R^- - W_R^-$ mediation

This contribution arising purely out of right-handed weak currents can also occur by the exchanges of $\hat{\nu}_i$, $\hat{S}_i$, and $\hat{N}_i$ and the corresponding diagrams are shown in Fig. 3.(a), Fig.

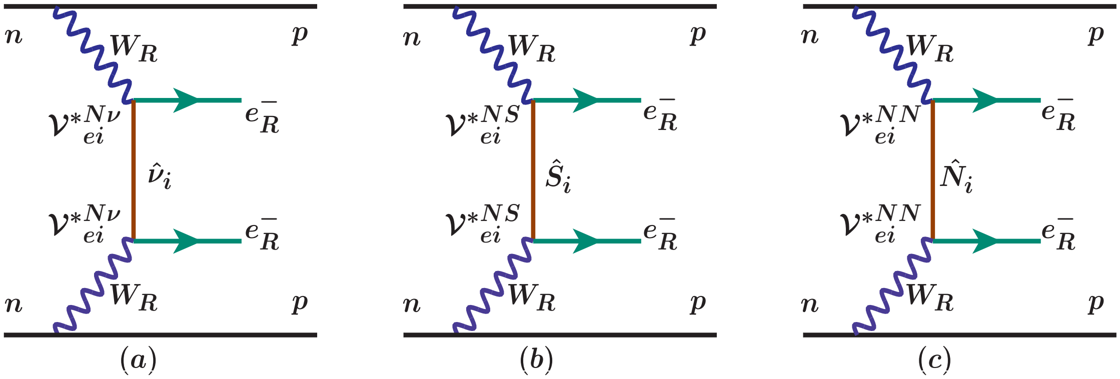

Figure 3: Same as Fig. 2 but with $W_R - W_R$ mediation.

3.(b), and Fig. 3.(c) leading to the amplitudes

$$\mathcal{A}_{\nu}^{RR} \propto \frac{1}{M_{W_R}^4}\frac{\left(\mathcal{V}_{e\,i}^{N\nu}\right)^2\, m_{\nu_i}}{p^2}\,, \tag{3.7}$$

$$\mathcal{A}_{S}^{RR} \propto \frac{1}{M_{W_R}^4}\frac{\left(\mathcal{V}_{e\,j}^{NS}\right)^2}{m_{S_j}}\,, \tag{3.8}$$

$$\mathcal{A}_{N}^{RR} \propto \frac{1}{M_{W_R}^4}\frac{\left(\mathcal{V}_{e\,j}^{NN}\right)^2}{m_{N_k}}\,. \tag{3.9}$$

3.3 $W_L^- - W_R^-$ mediation

According to our observation, although this contribution arising out of mixed effects by the exchanges of light LH and heavy RH neutrinos and also by the exchange of sterile neutrino is not so dominant compared to $W_L^- - W_L^-$ mediation with sterile neutrino exchanges as discussed in Sec. **3.1**, the amplitude is stronger than the standard one. The values of M contributing maximal effects in this case also gives maximal branching ratios for LFV decays. The light LH neutrinos and sterile neutrino exchange diagrams for this case are shown in Fig. 4.(a), Fig. 4.(b), and Fig. 4.(c), respectively, leading to the amplitudes

$$\mathcal{A}_{\nu}^{LR} \propto \frac{1}{M_{W_L}^2\, M_{W_R}^2}\left(\mathcal{V}_{e\,i}^{\nu\nu}\,\mathcal{V}_{e\,i}^{N\nu *}\right)\frac{1}{\not p}\,, \tag{3.10}$$

$$\mathcal{A}_{S}^{LR} \propto -\frac{1}{M_{W_L}^2\, M_{W_R}^2}\left(\mathcal{V}_{e\,i}^{\nu S}\mathcal{V}_{e\,i}^{NS *}\right)\frac{\not p}{\hat{m}_{S_i}}\,, \tag{3.11}$$

$$\mathcal{A}_{N}^{LR} \propto -\frac{1}{M_{W_L}^2\, M_{W_R}^2}\left(\mathcal{V}_{e\,i}^{\nu N}\mathcal{V}_{e\,i}^{\mathrm{NN} *}\right)\frac{\not p}{\hat{m}_{\mathcal{N}_k}}\,. \tag{3.12}$$

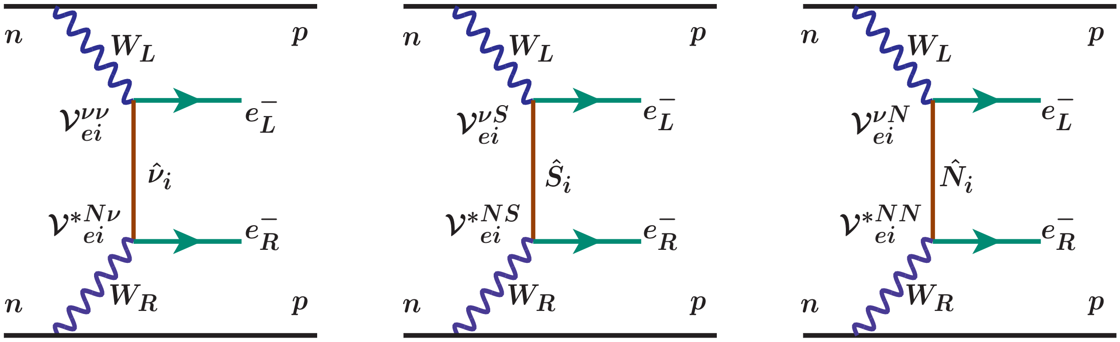

(a) (b) (c)

Figure 4: Same as Fig. 2 but with $W_L - W_R$ mediation.

3.4 Doubly Charged Higgs contribution

Although we have ignored contributions due to exchanges of LH (RH) doubly charged Higgs bosons Δ_L^{--} (Δ_R^{--}) in this work, we present the corresponding amplitudes for the sake of completeness,

(i) $\mathcal{A}^{LL}_{\Delta_L} \propto \frac{1}{M^4_{W_L}} \frac{1}{M^2_{\Delta_L}} f_L v_L$,

(ii) $\mathcal{A}^{RR}_{\Delta_R} \propto \frac{1}{M^4_{W_R}} \frac{1}{M^2_{\Delta_R}} f_R v_R$.

As stated in Sec. **2**, the masses of Δ_L^{--} and Δ_L^{++} are of the order of the large parity restoration scale which damps out the induced VEV v_L and the corresponding amplitude. The amplitude due to Δ_R^{--} exchange is damped out compared to the standard amplitude as it is $\propto \frac{1}{M^5_{W_R}}$.

3.5 Effective mass parameters

Including all relevant contributions except those due to doubly charged Higgs exchanges and using eq. (3.4)-(3.12), we express the inverse half-life in terms of effective mass parameters,

$$\frac{1}{T_{1/2}} = G_{0\nu} \frac{|\mathcal{M}_\nu|^2}{m_e^2} \left| M_{\rm ee}^{\bf tot} \right|^2 , \tag{3.13}$$

where $M_{\rm ee}^{\bf tot} = \sum_{k=1}^{9} M_{\rm ee}^{(\bf k)}$ and we have designated $M_{ee}^{(\bf k)}$ with $\mathbf{k} = 1, 2, 3$ as due to $W_L^- - W_L^-$ mediation, and those with $\mathbf{k} = 4, 5, 6$ and $\mathbf{k} = 7, 8, 9$ as due to $W_R^- - W_R^-$, and $W_L^- - W_R^-$ mediations, respectively. Analytic expression for all individual components are given in TABLE. 4:

$M_{\rm ee}^{(\bf 1)} = \sum_i \left(\mathcal{V}^{\nu\nu}_{e\,i}\right)^2 m_{\nu_i}$	$M_{\rm ee}^{(\bf 6)} = \sum_i \left(\frac{M_{W_L}}{M_{W_R}}\right)^4 \left(\mathcal{V}^{NN}_{e\,i}\right)^2 \frac{\lvert p\rvert^2}{m_{N_i}}$
$M_{\rm ee}^{(\bf 2)} = \sum_i \left(\mathcal{V}^{\nu S}_{e\,i}\right)^2 \frac{\lvert p\rvert^2}{m_{S_i}}$	$M_{\rm ee}^{(\bf 7)} = \sum_i \left(\frac{M_{W_L}}{M_{W_R}}\right)^2 \left(\mathcal{V}^{\nu\nu}_{e\,i} \mathcal{V}^{N\nu}\right) \lvert p\rvert$
$M_{\rm ee}^{(\bf 3)} = \sum_i \left(\mathcal{V}^{\nu N}_{e\,i}\right)^2 \frac{\lvert p\rvert^2}{m_{N_i}}$	$M_{\rm ee}^{(\bf 8)} = \sum_i \left(\frac{M_{W_L}}{M_{W_R}}\right)^2 \left(\mathcal{V}^{\nu S}_{e\,i} \mathcal{V}^{NS}\right) \frac{\lvert p\rvert^3}{m^2_{S_i}}$
$M_{\rm ee}^{(\bf 4)} = \sum_i \left(\frac{M_{W_L}}{M_{W_R}}\right)^4 \left(\mathcal{V}^{N\nu}_{e\,i}\right)^2 m_{\nu_i}$	$M_{\rm ee}^{(\bf 9)} = \sum_i \left(\frac{M_{W_L}}{M_{W_R}}\right)^2 \left(\mathcal{V}^{\nu N}_{e\,i} \mathcal{V}^{NN}\right) \frac{\lvert p\rvert^3}{m^2_{N_i}}$
$M_{\rm ee}^{(\bf 5)} = \sum_i \left(\frac{M_{W_L}}{M_{W_R}}\right)^4 \left(\mathcal{V}^{NS}_{e\,i}\right)^2 \frac{\lvert p\rvert^2}{m_{S_i}}$	

Table 4: The effective mass parameters $M_{ee}^{(\bf k)}$ due to $W_L^- - W_L^-$ mediation with $\mathbf{k} = 1, 2, 3$, $W_R^- - W_R^-$ mediation with $\mathbf{k} = 4, 5, 6$, and $W_L^- - W_R^-$ mediation with $\mathbf{k} = 7, 8, 9$ for the neutrinoless double beta decay.

4. Numerical estimation of effective mass parameters

Using analytic expression for $M_{\rm ee}^{(\bf k)}$, ($\mathbf{k} = 1, 2 ... 9$) given in Table. 4 and our model parameters discussed in Sec.**3**, we now estimate the relevant individual contributions numerically.

4.1 Nearly standard contribution

In our model the new mixing matrix $\mathcal{N}_{ei} \equiv \mathcal{V}^{\nu\nu}_{e\,i} = (1-\eta)\,U_\nu$ contains additional non-unitarity effect due to non-vanishing η where

$$\begin{aligned}
\mathcal{N}_{e1} &= (1-\eta_{e1})\,U_{11} - \eta_{e2}\,U_{21} - \eta_{e3}\,U_{31} \\
\mathcal{N}_{e2} &= (1-\eta_{e1})\,U_{12} - \eta_{e2}\,U_{22} - \eta_{e3}\,U_{32} \\
\mathcal{N}_{e3} &= (1-\eta_{e1})\,U_{13} - \eta_{e2}\,U_{23} - \eta_{e3}\,U_{33}
\end{aligned} \qquad (4.1)$$

We estimate numerical values of $\mathcal{N}_{ei}$ using all allowed values of η discussed in Sec.**2** and also by using $U \equiv U_{\rm PMNS}$. Then the effective mass parameter for nearly standard contribution $\sum_i \mathcal{N}^2_{e\,i}\, m_{\nu_i}$ is found to be almost similar to the standard prediction with $M^{(1)}_{ee} = 0.004\,(0.048)$ eV for NH (IH) light neutrino masses. This nearly standard prediction on effective mass parameter is presented by the green colored lines in the left-panels of Fig. 5 and Fig. 6 for the NH neutrino masses, but it is presented by the pink colored lines in the right panels of the same figures for the IH neutrino masses.

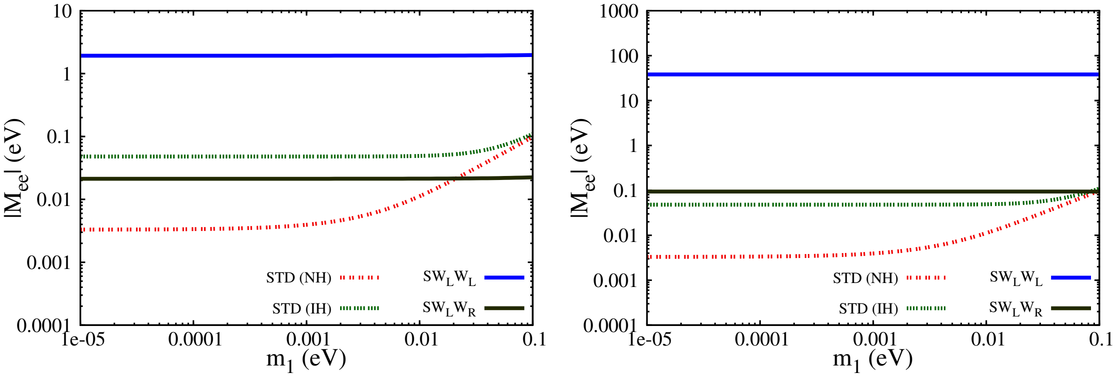

Figure 5: Variation of effective mass parameters with lightest light neutrino mass. The standard predictions are shown by dashed green (pink) colored lines for NH (IH) case. The non-standard contribution with $W^-_L - W^-_L$ mediation and sterile neutrino exchanges is shown by the upper blue solid line, whereas the one with $W^-_L - W^-_R$ mediation and sterile neutrino exchanges is shown by the lower black solid line.

In our numerical predictions, the left-panel of Fig. 5 is for M_D including RG corrections but with $M = (50, 200, 1172)$ GeV, $M_N = (1250, 3000, 5000)$ GeV, and $m_{\hat{S}} = (2, 13, 262)$ GeV whereas the right-panel of Fig. 5 corresponds to M_D excluding RG effects but for $M = (50, 200, 2495)$ GeV, $M_N = (1250, 3000, 5000)$ GeV, and $m_{\hat{S}} = (2, 13, 1035)$ GeV. Similarly, the left-panel of Fig. 6 is for M_D including RG corrections but with $M = (100, 100, 1286)$ GeV, $M_N = (5000, 5000, 5000)$ GeV, and $m_{\hat{S}} = (2, 2, 313)$ GeV whereas the right-panel of Fig. 6 corresponds to M_D excluding RG effects but for $M = (100, 100, 4877)$ GeV, $M_{\hat{N}} = (5000, 5000, 5000)$ GeV, and $m_{\hat{S}} = (2, 12, 2983)$ GeV.

4.2 Dominant non-standard contributions

Before estimating the effective mass parameters we present the mixing matrices numerically. As discussed in eq. (2.13) of Sec. **2**, the mixing matrices $X = M_D\, M^{-1}$, $Y = M\, M^{-1}_N$, $Z =$

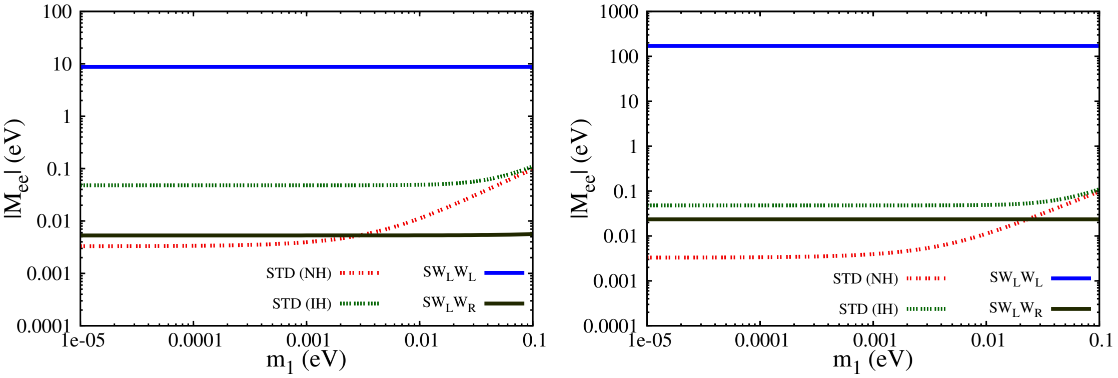

Figure 6: Variation of effective mass parameters with lightest light neutrino mass. The standard predictions are shown by dashed green (pink) colored lines for NH (IH) case. The non-standard contribution with $W_L^- - W_L^-$ mediation and sterile neutrino exchanges is shown by the upper blue solid line, whereas the one with $W_L^- - W_R^-$ mediation and sterile neutrino exchanges is shown by the lower black solid line.

$M_D\, M_N^{-1}$, and $y = \mu_S\, M^{-1}$ all contribute to non-standard predictions of $0\nu\beta\beta$ amplitude in the extended seesaw scheme.

Using eqn.(2.13) and the assumed diagonal structures of the RH Majorana neutrino mass matrix $M_N = \text{diag}(M_{N_1}, M_{N_2}, M_{N_3})$, $M = \text{diag}(M_1, M_2, M_3)$, and the Dirac neutrino mass matrix M_D, without or with RG corrections given in eq. (2.14) or eqn. (2.15), one can derive the relevant elements of the mixing matrices $\mathcal{N}$, $\mathcal{V}^{\nu N}$, $\mathcal{V}^{\nu S}$, $\mathcal{V}^{S\nu}$, $\mathcal{V}^{SS}$, $\mathcal{V}^{SN}$, $\mathcal{V}^{N\nu}$, $\mathcal{V}^{NS}$ and $\mathcal{V}^{NN}$ for which one example is

$$\begin{aligned}
&\mathcal{N}_{ei} = \{0.819, 0.552, 0.156\}\,, \qquad \mathcal{V}^{\nu S}_{ei} = \{6.7\times10^{-4}, 3\times10^{-3}, 1.5\times10^{-4}\}\,,\\
&\mathcal{V}^{\nu N}_{ei} = \{6.7\times10^{-5}, 3\times10^{-4}, 7.6\times10^{-5}\}\,, \quad \mathcal{V}^{S\nu}_{ei} = \{3.2\times10^{-3}, 3.0\times10^{-3}, 6.9\times10^{-3}\}\,,\\
&\mathcal{V}^{SS}_{ei} = \{0.999, 0.0002, 0.0001\},\ \mathcal{V}^{SN}_{ei} = \{0.1, 0.1, 0.5\},\ \mathcal{V}^{NN}_{ei} = \{1.0, 0.0, 0.0\}\,,\\
&\mathcal{V}^{N\nu}_{ei} = \{7.4\times10^{-7}, 1.8\times10^{-6}, 1.8\times10^{-6}\}\,, \qquad \mathcal{V}^{NS}_{ei} = \{0.1, 0.1, 0.5\}\,.
\end{aligned} \tag{4.2}$$

For evaluating these mixing elements we have taken the input values, M, M_N, and $\hat{m}_S$ presented under column **C1** of Table. 5 and M_D from eq. (2.14).

C1:	**C2:**
$M = \text{diag}\,(100.0, 100.0, 5000)$ GeV	$M = \text{diag}\,(20.0, 150.0, 3500)$ GeV
$M_N = \text{diag}\,(1000.0, 1000.0, 10000.0)$ GeV	$M_N = \text{diag}\,(200.0, 400.0, 10000.0)$ GeV
$\hat{m}_S = \text{diag}\,(10.0, 10.0, 2500)$ GeV	$\hat{m}_S = \text{diag}\,(2.0, 56.25, 1225)$ GeV
C3:	**C4:**
$M = \text{diag}\,(50.0, 200.0, 1172)$ GeV	$M = \text{diag}\,(100.0, 100.0, 1286.5)$ GeV
$M_N = \text{diag}\,(1250.0, 3000.0, 5000.0)$ GeV	$M_N = \text{diag}\,(5000.0, 5000.0, 5000.0)$ GeV
$\hat{m}_S = \text{diag}\,(2.0, 13.0, 362)$ GeV	$\hat{m}_S = \text{diag}\,(2.0, 2.0, 312)$ GeV .

Table 5: Input values of M, M_N, and $\hat{m}_S$ used for predicting effective mass parameters given in Table 6.

The numerical results for effective mass parameter contributing to $0\nu\beta\beta$ decay rate presented under column **C1** and **C2** (**C3** and **C4**) in TABLE. 6 are for Dirac neutrino mass matrix M_D of eq. (2.14) (eqn. (2.15)) excluding (including) RG effects where we have used the corresponding allowed solutions shown in Table. 5. It is clear that, RG effects while reducing the predicted values of M_D also reduce the predicted effective mass parameters for $0\nu\beta\beta$ in the relevant cases.

Effective mass parameter	**C1** (eV)	**C2** (eV)	**C3** (eV)	**C4** (eV)
$\lvert\mathbf{M}^{(1)}_{\rm ee}\rvert$	0.004	0.004	0.004	0.004
$\lvert\mathbf{M}^{(2)}_{\rm ee}\rvert$	34.0	206.2	1.93	7.0
$\lvert\mathbf{M}^{(3)}_{\rm ee}\rvert$	0.00389	0.07	$\simeq 0$	$\simeq 0$
$\lvert\mathbf{M}^{(4)}_{\rm ee}\rvert$	$\simeq 0$	$\simeq 0$	$\simeq 0$	$\simeq 0$
$\lvert\mathbf{M}^{(5)}_{\rm ee}\rvert$	0.0439	0.2197	0.0305	0.00768
$\lvert\mathbf{M}^{(6)}_{\rm ee}\rvert$	0.0435	0.2175	0.0308	0.00771
$\lvert\mathbf{M}^{(7)}_{\rm ee}\rvert$	0.127	0.124	0.0004	0.0004
$\lvert\mathbf{M}^{(8)}_{\rm ee}\rvert$	0.005	0.668	0.021	0.005
$\lvert\mathbf{M}^{(9)}_{\rm ee}\rvert$	$\simeq 0$	0.00007	$\simeq 0$	$\simeq 0$

Table 6: Predictions of effective mass parameter with the allowed model parameters. The results under **C1** and **C2** (**C3** and **C4**) are for the Dirac neutrino mass matrix excluding (including) RG corrections. The input values of mass matrices allowed by the current data for different columns are presented in Table 5.

The most dominant and new contribution to the effective mass parameters is found to emerge from the amplitude A^{LL}_S of eqn. (3.4) due to $W^-_L - W^-_L$ mediation and sterile

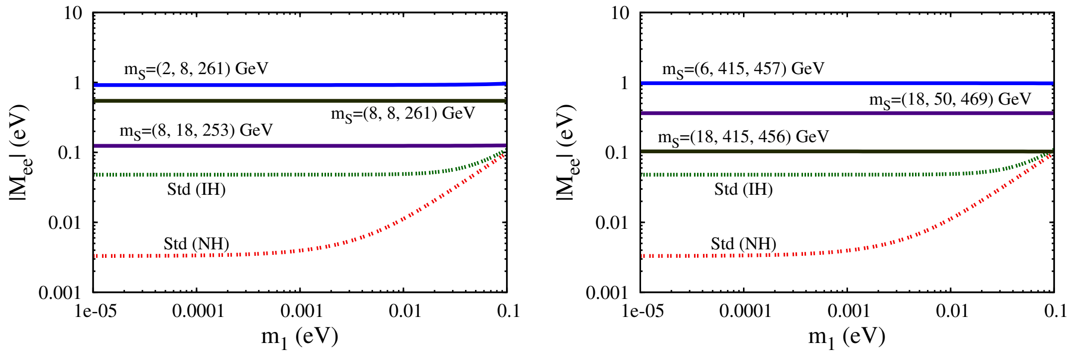

Figure 7: Predictions of non-standard contributions to effective mass parameter with $W^-_L - W^-_L$ mediation and sterile neutrino exchange for $M = (100, 200, 1169)$ GeV (top solid line), $M = (200, 200, 1168)$ GeV (middle solid line), and $M = (200, 300, 1150)$ GeV (bottom solid line) keeping $M_N = (5, 5, 5)$ TeV fixed and for M_D as in eq. (2.15) (*left-panel*). Similarly for the top, middle, and bottom solid lines $M = (170, 1500, 2181)$ GeV, $M = (300, 500, 2210)$ GeV, and $M = (300, 1500, 2179)$ GeV while keeping $M_N = (5, 5, 10)$ TeV fixed and for M_D as in eq. (2.14) (*right-panel*).

neutrino exchanges. This has been shown in Fig. 7 for various combinations of sterile neutrino mass eigenvalues where the left-panel (right-panel) is for M_D values including (excluding) RG corrections through eq. (2.15) (eq. (2.14)). In Fig. 7 our predictions range from 0.2 eV-1.0 eV. Looking to the results given in Table. 6 and Fig. 5, Fig. 6 , and Fig. 7, it is clear that the actual enhanced rate of $0\nu\beta\beta$ decay in this model depends primarily upon the sterile neutrino mass eigenvalues m_{S_1} and m_{S_2}. If the decay rate corresponds to $|M_{\rm eff}| \simeq 0.21 - 0.53$ eV as claimed by the Heidelberg-Moscow experiment using ^{76}Ge [11], our new finding is that the light neutrino masses could be still of NH or IH pattern but $m_{S_1} \sim 10\,\text{GeV}$ and $m_{S_2} \sim 20\,\text{GeV}$ if the Dirac neutrino mass matrix has high scale quark-lepton symmetric origin including RG corrections. The next dominant contributions coming from the Feynman amplitude A_S^{LR} of eqn. (3.12) due to $W_L^- - W_R^-$ mediation and sterile neutrino exchanges with $m_{ee}^{(8)} = 0.008$ eV (0.03 eV) have been shown in Fig. 5 and Fig. 6.

5. Predictions on lepton flavor violating decays and J$_{\rm CP}$

Besides the neutrinoless double beta decay process, the sterile and heavy neutrinos in this model can predominantly mediate different lepton flavor violating decays, $\mu \to e + \gamma$, $\tau \to e + \gamma$ and $\tau \to \mu + \gamma$. Since $\ell_\alpha \to \ell_\beta + \gamma$ $(\alpha \neq \beta)$ is lepton flavor changing process, it is strictly forbidden in the Standard Model when $m_\nu = 0$ and lepton number is conserved. In our model the underlying lepton-flavor violating interactions and non-unitarity effects contribute to LFV decays by the mediation of heavy RH Majorana and sterile Majorana fermions.

M(GeV)	M_N(TeV)	Heavy Mass Eigen Values(GeV)
(50, 200, 1172)	(1.25, 3, 5)	(1.99, 13.3, 262.3, 1251, 3013, 5262)
(100, 100,1286)	(5, 5, 5)	(1.99, 2.00, 312.8, 5002, 5002, 5313)
(100, 100,1286)	(5, 5, 10)	(1.99, 2.00, 163.5, 5002, 5002, 10164)
(100, 200,1169)	(5, 5, 5)	(1.99, 7.99, 261.1, 5002, 5008, 5261)
(1136, 1136, 1136)	(5, 5, 5)	(244.80,246.24,247.51,5246.2,5246.3,5247.5)

Table 7: The Heavy mass eigen values for the matrices of M and M_N which have been used to evaluate branching ratios.

5.1 Branching ratio

Keeping in mind the charged-current interaction in the neutrino mass basis for extended seesaw scheme given in eq. (3.1) - eq. (3.3), the dominant contributions are mainly through the exchange of the sterile and heavy RH neutrinos with branching ratio [24, 37]

$$\text{Br}\,(\ell_\alpha \to \ell_\beta + \gamma) = \frac{\alpha_{\rm w}^3\, s_{\rm w}^2\, m_{\ell_\alpha}^5}{256\,\pi^2\, M_W^4\, \Gamma_\alpha} \left|\mathcal{G}_{\alpha\beta}^N + \mathcal{G}_{\alpha\beta}^S\right|^2 , \tag{5.1}$$

$$\text{where} \quad \mathcal{G}^N_{\alpha\beta} = \sum_k \left(\mathcal{V}^{\nu\, N}\right)_{\alpha\, k} \left(\mathcal{V}^{\nu\, N}\right)^*_{\beta\, k} \mathcal{I}\left(\frac{m^2_{N_k}}{M^2_{W_L}}\right) ,$$

$$\mathcal{G}^S_{\alpha\beta} = \sum_j \left(\mathcal{V}^{\nu\, S}\right)_{\alpha\, j} \left(\mathcal{V}^{\nu\, S}\right)^*_{\beta\, j} \mathcal{I}\left(\frac{m^2_{S_j}}{M^2_{W_L}}\right) ,$$

$$\text{and} \quad \mathcal{I}(x) = -\frac{2x^3 + 5x^2 - x}{4(1-x)^3} - \frac{3x^3 \ln x}{2(1-x)^4} .$$

It is clear from the above equation and within the model parameter range allowed in our theory, $M_N \gg M \gg M_D$, that the first term in eq. (5.1) is negligible while second term involving the the heavy sterile neutrinos gives dominant contributions which is proportional to $\sum_j \left(\mathcal{V}^{\nu\, S}\right)_{\alpha\, j} \left(\mathcal{V}^{\nu\, S}\right)^*_{\beta\, j} \simeq 2\eta_{\alpha\beta}$.

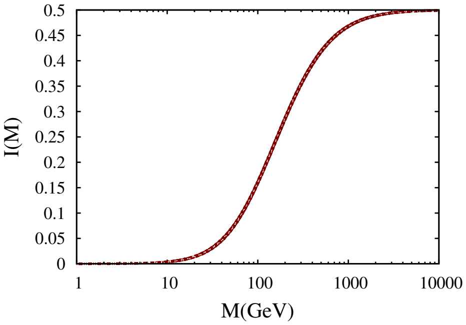

Figure 8: Loop factor vs masses of heavy RH or sterile neutrino.

Taking into account the contribution of the non-unitarity matrix, it is clear that out of diagonal elements of M_N and M, mostly the latter contributes to the branching ratios. Also the contribution of loop factor for various range of masses allowed in this extended seesaw mechanism is shown in Fig. 8.

M(GeV)	M_N(TeV)	Br($\mu \to e\gamma$)	Br($\tau \to e\gamma$)	Br($\tau \to \mu\gamma$)
(50, 200, 1172)	(1.25, 3, 5)	2.0×10^{-16}	2.1×10^{-14}	3.0×10^{-12}
(100, 100, 1286)	(5, 5, 5)	1.6×10^{-16}	1.7×10^{-14}	2.4×10^{-12}
(100, 100, 1286)	(5, 5, 10)	7.4×10^{-17}	8.2×10^{-15}	1.1×10^{-12}
(100, 200, 1169)	(5, 5, 5)	2.0×10^{-16}	2.1×10^{-14}	3.0×10^{-12}
(1136,1136,1136)	(5,5,5)	2.1×10^{-16}	2.3×10^{-14}	3.2×10^{-12}

Table 8: The three branching ratios in extended inverse seesaw for different values of M and M_N while M_D is same as in eq. 2.15.

Using the numerically computed mixing matrix, our model predictions on branching ratios are given in Table 8. Recent experimental data gives the best limit on these branching ratios for LFV decays coming from the MEG collaboration [38]. Among these $\text{Br}\,(\mu \to e + \gamma) \leq 1.2 \times 10^{-11}$ [38] is almost three orders of magnitude stronger than the limit $\text{Br}\,(\tau \to e + \gamma) \leq 3.3 \times 10^{-8}$ or $\text{Br}\,(\tau \to \mu + \gamma) \leq 4.4 \times 10^{-8}$ at 90% C.L. However, projected reach of future sensitivities of ongoing searches are $\text{Br}\,(\tau \to e + \gamma) \leq$

10^{-9}, $\mathrm{Br}\left(\tau \rightarrow \mu+\gamma\right) \leq 10^{-9}$, and $\mathrm{Br}\left(\mu \rightarrow e+\gamma\right) \leq 10^{-18}$ [38] which might play crucial role in verifying or falsifying the discussed scenario.

5.2 CP-violation due to non-unitarity

There are attempts taken in long baseline experiments [13] with accelerator neutrinos ν_μ and anti-neutrons $\bar{\nu}_\mu$ to search for CP violating effects in neutrino oscillations. In the usual notation, the standard contribution to these effects is determined by the rephasing invariant $J_{\rm CP}$ associated with the Dirac phase δ_{CP} and matrix elements of the PMNS matrix

$$J_{\rm CP} \equiv \mathrm{Im}\left(U_{\alpha\, i} U_{\beta\, j} U^*_{\alpha\, j} U^*_{\beta\, j}\right) = \cos\theta_{12}\, \cos^2\theta_{13}\, \cos\theta_{23}\, \sin\theta_{12}\, \sin\theta_{13}\, \sin\theta_{23}\, \sin\delta_{\rm CP}.$$

In this extended seesaw mechanism, the leptonic CP-violation can be written as

$$\mathcal{J}^{ij}_{\alpha\beta} = \mathrm{Im}\left(\mathcal{N}_{\alpha\, i} \mathcal{N}_{\beta\, j} \mathcal{N}^*_{\alpha\, j} \mathcal{N}^*_{\beta\, j}\right) \simeq J_{\rm CP} + \Delta J^{ij}_{\alpha\beta} \tag{5.2}$$

where [30, 31, 33, 34]

$$\begin{aligned} \Delta J^{ij}_{\alpha\beta} = - \sum_{\rho = e,\mu,\tau} \; \mathrm{Im}\Big[& \eta_{\alpha\rho}\, U_{\rho i}\, U_{\beta j}\, U^*_{\alpha j}\, U^*_{\beta i} + \eta_{\beta\rho}\, U_{\alpha i}\, U_{\rho j}\, U^*_{\alpha j}\, U^*_{\beta i} \\ & + \eta^*_{\alpha\rho}\, U_{\alpha i}\, U_{\beta j}\, U^*_{\rho j}\, U^*_{\beta j} + \eta^*_{\beta\rho}\, U_{\alpha i}\, U_{\beta j}\, U^*_{\alpha j}\, U^*_{\rho j} \Big]. \end{aligned} \tag{5.3}$$

The extra contribution arises because of the non-unitarity mixing matrix which depends on both M_D and M. Thus the new contribution to CP-violation is larger for larger M_D which is generated with quark-lepton symmetry and for smaller M while safeguarding the constraint $M_N \gg M > M_D, \mu_S$. It is noteworthy that in our model even if the leptonic Dirac phase $\delta_{\rm CP} \simeq 0, \pi, 2\pi$, and/or $\sin\theta_{13} \rightarrow 0$, there is substantial contribution to CP-violation which might arise out of the imaginary parts of the non-unitarity matrix elements $\eta_{\alpha\beta}$.

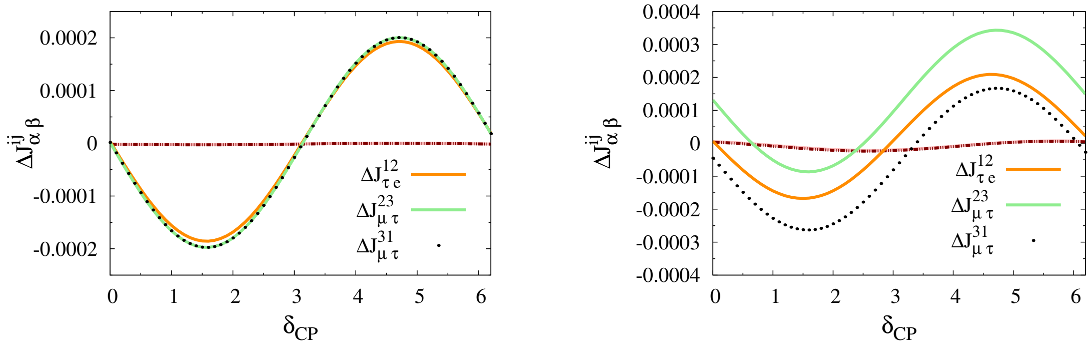

Figure 9: CP-violation for the full allowed range of leptonic Dirac phase δ_{CP}. The left-panel corresponds to degenerate values of M with $M_1 = M_2 = M_3 \simeq 1137$ GeV, and the right panel is due to non-degenerate M with $M_1 = 6.8$ GeV, $M_2 = 81.5$ GeV, and $M_3 = 1962$ GeV.

M	$\Delta\mathcal{J}^{12}_{e\mu}$	$\Delta\mathcal{J}^{23}_{e\mu}$	$\Delta\mathcal{J}^{23}_{\mu\tau}$	$\Delta\mathcal{J}^{31}_{\mu\tau}$	$\Delta\mathcal{J}^{12}_{\tau e}$
(a)	-2.0×10^{-6}	-2.3×10^{-6}	-1.2×10^{-4}	-1.2×10^{-4}	-1.1×10^{-4}
(b)	-2.7×10^{-6}	-3.2×10^{-6}	-1.2×10^{-4}	-1.2×10^{-4}	-1.1×10^{-4}
(c)	-2.1×10^{-5}	-2.4×10^{-5}	1.1×10^{-7}	-1.8×10^{-4}	-7.9×10^{-5}

Table 9: The CP-violating effects for (a) degenerate masses $M = (1137, 1137, 1137)$ GeV, (b) partially degenerate masses $M = (100, 100, 1286)$ GeV and (c) non degenerate masses $M = (6.85, 81.1, 1967)$ GeV, while M_D is same as in eq. (2.15).

Our estimations using RG corrected Dirac neutrino mass matrix and both degenerate and non-degenerate matrix M are shown in the left-panel and right-panel of Fig. 9. If the leptonic Dirac phase $\delta_{\rm CP} \neq 0, \pi, 2\pi$, significant CP-violation up to $|\Delta\, J|_{\rm max} \simeq 1.5\times10^{-4}$ is found to occur for degenerate M, but when M is non-degenerate we obtain $|\Delta\, J|_{\rm max} \simeq (2-4)\times10^{-4}$. Also even if $\delta_{\rm CP} \simeq 0, \pi, 2\pi$, non-vanishing CP-violation to the extent of $|\Delta\, J| \simeq (1-2)\times10^{-4}$ is predicted for non-degenerate M. These results may be compared with CP-violation in the quark sector where $\mathcal{J}_{\rm CKM} \simeq 3.05^{+0.19}_{-0.20}\times10^{-5}$ [28] which is nearly one order lower than the leptonic case. The horizontal lines in Fig. 9 represent absence of non-unitarity effects on CP-violation.

6. Implementation in SO(10)

Our main goal in this section is to examine whether the TeV scale LR gauge model that has been shown to give rise to dominant contribution to $0\nu\beta\beta$ decay and lepton flavor violation in Secs. **2-5** can emerge from a non-SUSY $SO(10)$ grand unified theory. Although the search for low mass $W_R^{\pm}$ bosons in non-SUSY GUTs has been attempted initially without [39] precision CERN-LEP data on $\alpha_S(M_Z)$ and $\sin^2\theta_W(M_Z)$ [28], there are more recent results on physically appealing intermediate scales [40, 41]. But the analyses in non-SUSY cases where the $B-L$ breaking scale synonymous to W_R gauge boson mass much lower than 10^{10} GeV are ruled out because of the associated large contributions to light neutrino masses via type-I seesaw mechanism. In view of the rich phenomenological consequences of the extended seesaw mechanism that evades the discordance between dominant $0\nu\beta\beta$ decay and small neutrino mass predictions as discussed in Sec.**2-5**, we explore the possibility of such low scale LR gauge theory in the minimally extended $SO(10)$ grand unification model.

6.1 Symmetry breaking chain

We consider the symmetry breaking chain discussed in Ref. [41] which, as such, is now ruled out because of the TeV scale canonical seesaw that operates to give large neutrino masses in contravention of the oscillation data. Now we modify this model by including the additional doublets $(\chi_L, \chi_R) \subset 16_H$ of $SO(10)$ and extending the minimal fermion content in $\{16\}_F$ with the addition of one $SO(10)$ singlet neutral fermion per generation in order to implement the extended seesaw mechanism

$$\begin{aligned}
SO(10) \quad & \xrightarrow[\{54\}]{M_U} SU(2)_L \times SU(2)_R \times SU(4)_C \times D \qquad [\mathcal{G}_{224D},\ (g_{2L}=g_{2R})] \\
& \xrightarrow[\{210\}]{M_P} SU(2)_L \times SU(2)_R \times SU(4)_C \qquad [\mathcal{G}_{224},\ (g_{2L}\neq g_{2R})] \\
& \xrightarrow[\{45\}]{M_C} SU(2)_L \times SU(2)_R \times U(1)_{B-L} \times SU(3)_C \qquad [\mathcal{G}_{2213}\,] \\
& \xrightarrow[\{210\}]{M_R^+} SU(2)_L \times U(1)_R \times U(1)_{B-L} \times SU(3)_C \qquad [\mathcal{G}_{2213}\,] \\
& \xrightarrow[\{126\}]{M_R^0} SU(2)_L \times U(1)_Y \times SU(3)_C \qquad [\mathcal{G}_{\rm SM}\,] \\
& \xrightarrow[\{10\}]{M_Z} U(1)_{\rm em} \times SU(3)_C .
\end{aligned} \tag{6.1}$$

It is well known [17] that the triplets $(\Delta_L, \Delta_R) \subset \{126\}_H$ and the bidoublet $\Phi \subset \{10\}_H$ of $SO(10)$. It was also found that the G_{224}-singlets in $\{54\}_H$ and $\{210\}_H$ of $SO(10)$ are D-parity even and odd, respectively. Also it was noted that the neutral components of the G_{224} multiplet $\{1, 1, 15\}$ contained in $\{210\}_H$ and $\{45\}_H$ of $SO(10)$ have D-parity even and odd, respectively. In the first step, VEV is assigned along the $\langle(1, 1, 1)\rangle \subset \{54\}_H$ to guarantee the LR symmetric Pati-Salam group to survive while at the second step D-parity is broken by assigning $\langle(1, 1, 1)\rangle \subset \{210\}_H$ to obtain asymmetric G_{224} with $g_{2L} \neq g_{2R}$. The spontaneous breaking $G_{224} \to G_{2213}$ is achieved by the VEV $\langle(1, 1, 15)^0_H\rangle \subset \{45\}_H$. The symmetry breaking $G_{2213} \to G_{2113}$ is implemented by the sub-multiplet $\langle(1, 3, 15)^0_H\rangle \subset \{210\}_H$, and $U(1)_R \times U(1)_{B-L} \to U(1)_Y$ is achieved by $\langle\Delta^0_R\rangle \subset \{126\}_H$ while the VEV $\langle\chi^0_R\rangle \subset \{16\}_H$ provides the N-S mixing. As usual, the breaking of SM to low energy symmetry $U(1)_{em} \times SU(3)_C$ is carried out by the SM doublet contained in the bidoublet $\Phi \subset \{10\}_H$.

6.2 Gauge coupling unification

The one-loop and two-loop coefficients of β-functions of renormalization group equations for the gauge couplings [42]

$$\mu \frac{\partial g_i}{\partial \mu} = \frac{a_i}{16\pi^2} g_i^3 + \frac{1}{16\pi^2} \sum_j b_{ij} g_i^3 g_j^2 \,, \tag{6.2}$$

M_R^0 (TeV)	M_R^+ (TeV)	M_C (TeV)	M_P (GeV)	M_G (GeV)	α_G
1	10	10^3	$10^{14.17}$	$10^{17.79}$	0.0388
1	10	10^4	$10^{14.59}$	$10^{17.74}$	0.0350
1	10	$10^{4.5}$	$10^{14.80}$	$10^{17.72}$	0.0335
1	1.259	10^4	$10^{14.96}$	$10^{18.05}$	0.0342
1	1.259	10^3	$10^{14.54}$	$10^{18.10}$	0.0378

Table 10: The gauge coupling at the unification with predicted D-parity preserving Pati-Salam scale and unification scale for assumed set of M_R^0, M_R^+, and M_C scales.

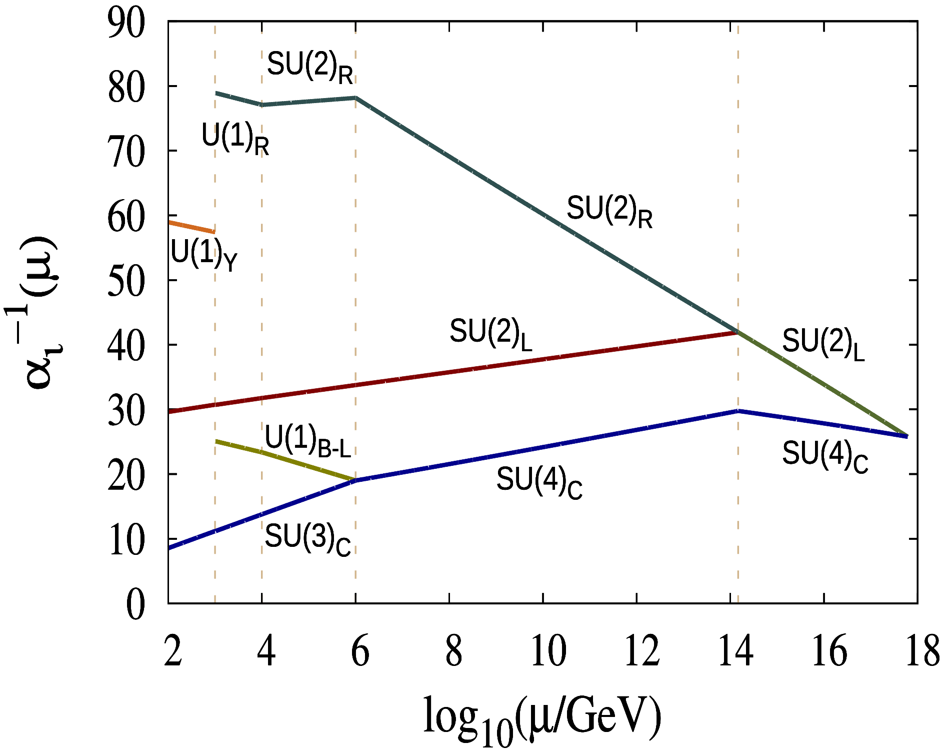

Figure 10: Two loop gauge coupling unification.

are given in Table. 11 of appendix. Using precision CERN-LEP data [28] $\alpha_S(M_Z) = 0.1184$, $\sin^2\theta_W(M_Z) = 0.2311$ and $\alpha^{-1}(M_Z) = 127.9$, different allowed solutions presented in Table. 10. One set of solutions corresponding to low mass $W_R^{\pm}$ and Z_R gauge bosons is

$$\begin{aligned} M_R^0 = 1 \text{ TeV}, \; M_R^+ = 10 \text{ TeV}, \; M_C = 10^2 \text{ TeV} - 10^3 \text{ TeV}\,, \\ M_P \simeq 10^{14.17} \text{ GeV and } M_{\text{GUT}} \simeq 10^{17.8} \text{ GeV}. \end{aligned} \tag{6.3}$$

For these mass scales the emerging pattern of gauge coupling unification is shown in Fig. 10 with GUT fine structure constant $\alpha_G = 0.0388$.

6.3 Physical significance of mass scales

The presence of G_{224D} symmetry above the highest intermediate scale plays a crucial role in lowering down the values of M_R^+ while achieving high scale gauge coupling unification. These low mass W_R and Z_R bosons have interesting RH current effects at low energies including K_L-K_S mass difference and dominant $0\nu\beta\beta$ rates as discussed in Sec. **3-5**. The predicted low mass $W_R^{\pm}$ and Z_R bosons are also expected to be testified at the LHC and future accelerators for which the current bounds are $M_{W_R} \geq 2.2$ TeV and $M_{Z_R} \geq 1$ TeV [20]. The predicted mass scale $M_C \sim \left(10^5 - 10^6\right)$ GeV leads to experimentally verifiable branching ratios for rare kaon decay with $\text{Br}(K_L^0 \to \mu\bar{e}) \simeq \left(10^{-9} - 10^{-11}\right)$ [23]

via leptoquark gauge boson mediation. Because of the presence of $\mathcal{G}_{224}$ symmetry for $\mu \geq M_C \left(10^5 - 10^6\right)$ GeV, all the components of diquark Higgs scalars in $\Delta_R(3,1,\bar{10})$ mediating $n - \bar{n}$ and $H - \bar{H}$ oscillations also acquire masses at that scale whereas the dilepton Higgs scalar carrying $B - L = -2$ is at the $\simeq 1$ TeV scale. This gives rise to observable $n - \bar{n}$ oscillation with mixing time $\tau_{n-\bar{n}} \simeq \left(10^8 - 10^{11}\right)$ secs [22, 43]. However because of the large value of the GUT scale $M_G \simeq 10^{18}$ GeV, which is close to the Planck scale, the predicted proton life time for $p \to e^+\pi^0$ is large, i.e. $\tau_{\mathrm{p}} \geq 10^{40}$ yrs which is beyond the accessible range of ongoing search experiments that have set the lower limit $(\tau_{\mathrm{p}})\big|_{\mathrm{expt.}} \geq 1.1 \times 10^{34}$ yrs [44].

6.4 Importance of $\mathcal{G}_{224D}$ intermediate symmetry

Near Planck scale unification of this model exposes an interesting possibility that grand unification can be also achieved by the Pati-Salam symmetry $\mathcal{G}_{224D}$ even without the help of the GUT-gauge group SO(10) since, above this scale, gravity effects are expected to take over [45].

The most interesting role of G_{224D} gauge symmetry at the highest intermediate scale has been pointed out in Ref. [46]. Normally super-heavy Higgs scalars contained in larger representations like $\{210\}_H$ and $\{126\}_H$ introduce uncertainties into GUT predictions of $\sin^2\theta_W(M_Z)$ on which CERN-LEP data and others have precise experimental results. But the presence of G_{224D} at the highest scale achieves the most desired objective that the GUT scale corrections to $\sin^2\theta_W(M_Z)$ vanish due to such sources as super-heavy particles or higher dimensional operators signifying the effect of gravity.

6.5 Prediction of Dirac neutrino mass matrix

It is well known that within Pati-Salam gauge symmetry $\mathcal{G}_{224D}$, the presence of $SU(4)_C$ unifies quarks and leptons treating the latter as fourth color. This leads to the prediction $M_u \simeq M_D$ at the unification scale. This relation is also valid in $SO(10)$ at the GUT scale since $\mathcal{G}_{224D}$ is its maximal subgroup. In view of this, it is important to examine the extent of validity of $M_u \simeq M_D$ at low scales as has been assumed in deriving eqn.(2.14). This question has been answered in non-SUSY $SO(10)$ [31] and SUSY $SO(10)$ [30] while utilizing renormalization group running of fermion masses analogous to ref. [29] and using their low energy data where [30, 31] both the bottom-up and top-down approaches have been used. The present non-supersymmetric $SO(10)$ model is expected to yield M_D value at $\mu \simeq M_Z$ similar to eqn.(2.15). For the sake of completeness in all our analyses on $0\nu\beta\beta$ decay predictions in Sec.**3-4**, we have given estimations of effective mass parameters using both eqn.(2.15) and eqn.(2.14) by excluding or including such RG corrections.

7. Summary and Conclusion

In this work we have investigated in detail the prospects of TeV scale left-right gauge theory with high scale parity restoration suitably modified to implement extended seesaw mechanism in predicting dominant contributions to $0\nu\beta\beta$ decay. We have also embedded the model successfully in non-SUSY $SO(10)$ GUT predicting low mass $W_R^{\pm}$ and Z_R bosons near the TeV scale accessible to Large Hadron Collider (LHC) and future accelerators. We have shown that low mass $W_R^{\pm}$ and Z_R bosons, and dominant contributions to $0\nu\beta\beta$ decay are in concordance with the oscillation data for explaining tiny masses of light neutrinos which are governed by a gauged inverse seesaw formula. A major role of the sterile neutrinos, generically required in such inverse seesaw mechanism, that has been found for the first time in this work is that they predict most dominant contributions to the $0\nu\beta\beta$ decay rate with effective mass parameter value $M_{\rm ee}^{(\mathbf{2})} \equiv M_{\rm ee}^{\rm sterile} \simeq (0.5-7)$ eV in the $W_L^- - W_L^-$ mediated channel. In addition, the next dominant contribution in the $W_L^- - W_R^-$ mediated channel due to the exchanges of light and heavy RH neutrinos and sterile neutrinos has been also found. The quark-lepton symmetric origin of the Dirac neutrino mass matrix is also found to play a crucial role in enhancing $0\nu\beta\beta$ decay rate, and non-unitarity effects leading to enhanced lepton flavor violations and leptonic CP-violation. Even with negligible unitarity CP-violating Dirac phases $\delta_{\rm CP} \simeq 0, \pi, 2\pi$, the model predict non-unitarity CP-violation larger than the quark sector.

The prediction of $W_R^{\pm}$ and Z_R bosons in this particular non-SUSY $SO(10)$ GUT theory is further accompanied by observable $n-\bar{n}$ oscillation with mixing time $\tau_{n-\bar{n}} \simeq \left(10^8 - 10^{11}\right)$ secs as well as lepto-quark gauge boson mediated rare kaon decay with ${\rm Br}\left(K_{\rm L} \to \mu\bar{e}\right) \simeq \left(10^{-9} - 10^{-11}\right)$ accessible to ongoing experiments. Another set of important predictions of LR and $SO(10)$ GUT models is noted to include non-unitarity effects and branching ratios for LFV decays with ${\rm Br}\left(\tau \to e+\gamma\right) = 2.0 \times 10^{-14}$, ${\rm Br}\left(\tau \to \mu+\gamma\right) \leq 2.8 \times 10^{-12}$, and ${\rm Br}\left(\mu \to e+\gamma\right) \leq 2.5 \times 10^{-16}$ accessible to ongoing searches.

We conclude that the experimentally verifiable extended seesaw mechanism in conjunction with TeV scale asymmetric left-right gauge theory accessible to high energy accelerators provides a rich structure of weak interaction phenomenology including light neutrino masses, neutrinoless double beta decay, non-unitarity effects, and CP-violation. These can originate from an $SO(10)$ grand unified theory with additional verifiable signatures like $n-\bar{n}$ oscillation and rare kaon decays. In particular, our finding on sterile neutrino mediated dominant $0\nu\beta\beta$ decay rate in the $W_L^- - W_L^-$ channel suggests that the Heidelberg-Moscow experimental data could be consistent with light active neutrino masses.

A. APPENDIX

The main goal of this section is to derive the masses and mixings for the neutrino sector in the extended seesaw mechanism which plays a prime role in determining lepton flavor violating processes like $0\nu\beta\beta$ decay rate as well as branching ratios for the lepton flavor violating decays. To start with, let us write the complete mass matrix for extended seesaw model in flavor basis $\{\nu_L, S_L, N_R^C\}$ as

$$\mathcal{M}_\nu = \begin{pmatrix} 0 & 0 & M_D \\ 0 & \mu_S & M^T \\ M_D^T & M & M_N \end{pmatrix} \tag{A.1}$$

The flavor basis to mass basis transformation and the diagonalization of the above mass matrix is achieved through a unitary matrix

$$|\psi\rangle_f = \mathcal{V}\,|\psi\rangle_m \tag{A.2}$$

$$\text{or,}\quad \begin{pmatrix} \nu_\alpha \\ S_\beta \\ N^C_\gamma \end{pmatrix} = \begin{pmatrix} \mathcal{V}^{\nu\nu}_{\alpha i} & \mathcal{V}^{\nu S}_{\alpha j} & \mathcal{V}^{\nu N}_{\alpha k} \\ \mathcal{V}^{S\nu}_{\beta i} & \mathcal{V}^{SS}_{\beta j} & \mathcal{V}^{SN}_{\beta k} \\ \mathcal{V}^{N\nu}_{\gamma i} & \mathcal{V}^{NS}_{\gamma j} & \mathcal{V}^{NN}_{\gamma k} \end{pmatrix} \begin{pmatrix} \hat{\nu}_i \\ \hat{S}_j \\ \hat{N}_k \end{pmatrix} \tag{A.3}$$

$$\text{and}\;\; \mathcal{V}^\dagger \mathcal{M}_\nu \mathcal{V}^* = \hat{\mathcal{M}}_\nu = \text{diag}\left(\hat{m}_{\nu_i}; \hat{m}_{\mathcal{S}_j}; \hat{m}_{\mathcal{N}_k}\right) \tag{A.4}$$

where subscripts f, m denote for the flavor and mass basis, respectively. Also $\mathcal{M}_\nu$ is the mass matrix in flavor basis with α, β, γ run over three generations of light-neutrinos, sterile-neutrinos and right handed heavy-neutrinos in flavor state whereas $\hat{\mathcal{M}}_\nu$ is the diagonal mass matrix with $(i, j, k = 1, 2, 3)$ run over corresponding mass states at the sub-eV, GeV and TeV scales, respectively.

Before proceeding to diagonalize the mass matrix, the mass hierarchy $M_N \gg M > M_D, \mu_S$ as well as $\mu_S\, M_N < M^2$ has been assumed in our model. The method of complete diagonalization will be carried out by two step: (**1**) the full neutrino mass matrix $\mathcal{M}_\nu$ has to reduced to a block diagonalized form as $\mathcal{M}_{\text{BD}}$, (**2**) this block diagonal form further diagonalized to give physical masses of the neutral leptons $\hat{\mathcal{M}}_\nu$.

A.1 Block diagonalization and determination of $\mathcal{M}_{\text{BD}}$

We shall follow the parameterization of type given in Ref. [27] to determine the form of $\mathcal{W}$. In order to evaluate $\mathcal{W}$, let us decompose $\mathcal{W}$ as $\mathcal{W} = \mathcal{W}_1\, \mathcal{W}_2$ where $\mathcal{W}_1$ and $\mathcal{W}_2$ satisfy

$$\mathcal{W}_1^\dagger \mathcal{M}_\nu \mathcal{W}_1^* = \hat{\mathcal{M}}_{\text{BD}}, \text{and} \quad \mathcal{W}_2^\dagger \hat{\mathcal{M}}_{\text{BD}} \mathcal{W}_2^* = \mathcal{M}_{\text{BD}} \tag{A.5}$$

where $\hat{\mathcal{M}}_{\text{BD}}$, and $\mathcal{M}_{\text{BD}}$ are the intermediate block-diagonal, and full block-diagonal mass matrices, respectively,

$$\hat{\mathcal{M}}_{\text{BD}} = \begin{pmatrix} \mathcal{M}_{eff} & 0 \\ 0 & m_{\mathcal{N}} \end{pmatrix} \tag{A.6}$$

$$\text{and}\;\; \mathcal{M}_{\text{BD}} = \begin{pmatrix} m_\nu & 0 & 0 \\ 0 & m_{\mathcal{S}} & 0 \\ 0 & 0 & m_{\mathcal{N}} \end{pmatrix} \tag{A.7}$$

A.1.1 Determination of $\mathcal{W}_1$

We need to first integrate out the heavy state (N_R), being heavier than other mass scales in our theory, such that up to the leading order approximation the analytic expressions for $\mathcal{W}_1$ is

$$\mathcal{W}_1 = \begin{pmatrix} 1 - \frac{1}{2} B^* B^T & B^* \\ -B^T & 1 - \frac{1}{2} B^T B^* \end{pmatrix}, \tag{A.8}$$

where the matrix B is 6×3 dimensional and is described as

$$B^\dagger = M_N^{-1}\left(M_D^T, M^T\right) = \left(Z^T, Y^T\right) \tag{A.9}$$

where, $X = M_D M^{-1}$, $Y = M M_N{}^{-1}$, and $Z = M_D M_N^{-1}$ so that $Z = X \cdot Y \neq Y \cdot X$ and $y = M^{-1}\mu_S$, $z = M_N^{-1}\mu_S$.

Therefore, the transformation matrix $\mathcal{W}_1$ can be written purely in terms of dimensionless parameters Y and Z

$$\mathcal{W}_1 = \begin{pmatrix} 1-\frac{1}{2}ZZ^\dagger & -\frac{1}{2}ZY^\dagger & Z \\ -\frac{1}{2}YZ^\dagger & 1-\frac{1}{2}YY^\dagger & Y \\ -Z^\dagger & -Y^\dagger & 1-\frac{1}{2}(Z^\dagger Z + Y^\dagger Y) \end{pmatrix} \tag{A.10}$$

while the light and heavy states can be now written as

$$\mathcal{M}_{eff} = \begin{pmatrix} 0 & 0 \\ 0 & \mu_S \end{pmatrix} - \begin{pmatrix} M_D M_N^{-1} M_D^T & M_D M_N^{-1} M^T \\ M M_N^{-1} M_D^T & M M_N^{-1} M^T \end{pmatrix} \tag{A.11}$$

$$m_{\mathcal{N}} = M_N + .. \tag{A.12}$$

A.1.2 Determination of $\mathcal{W}_2$

From the above discussion, it is quite clear now that the eigenstates $\mathcal{N}_i$ are eventually decoupled from others and the remaining mass matrix $\mathcal{M}_{eff}$ can be block diagonalized using another transformation matrix

$$\mathcal{S}^\dagger \mathcal{M}_{\rm eff} \mathcal{S}^* = \begin{pmatrix} m_\nu & 0 \\ 0 & m_{\mathcal{S}} \end{pmatrix} \tag{A.13}$$

such that

$$\mathcal{W}_2 = \begin{pmatrix} \mathcal{S} & 0 \\ 0 & 1 \end{pmatrix} \tag{A.14}$$

In a simplified structure

$$-\mathcal{M}_{eff} = \begin{pmatrix} M_D Z^T & M_D Y^T \\ Y M_D^T & (M Y^T - \mu_S) \end{pmatrix} \tag{A.15}$$

Under the assumption at the beginning $Z << Y$, and of-course $M_D << M$, this structure is similar to type-(I+II) seesaw. Therefore we immediately get the light neutrino masses as

$$\begin{aligned} m_\nu &= -M_D Z^T + M_D Y^T (M Y^T - \mu_S)^{-1} Y M_D^T \\ &= -M_D Z^T + M_D Z^T + M_D M \mu_S (Z Y^{-1})^T \\ &= M_D M^{-1} \mu_S (M_D M^{-1})^T \end{aligned} \tag{A.16}$$

$$m_{\mathcal{S}} = \mu_S - M M_N^{-1} M^T \tag{A.17}$$

We see that in addition to $m_{\mathcal{N}}$ the $m_{\mathcal{S}}$ is also almost diagonal if M and M_N are assumed to be diagonal. The transformation matrix S is

$$S = \begin{pmatrix} 1-\frac{1}{2}A^* A^T & A^* \\ -A^T & 1-\frac{1}{2}A^T A^* \end{pmatrix} \tag{A.18}$$

such that

$$\begin{aligned} A^\dagger &= (MY^T - \mu_S)^{-1} Y M_D^T \\ &\simeq (MY^T)^{-1} Y M_D^T = X^T \,. \end{aligned} \tag{A.19}$$

The 3×3 block diagonal mixing matrix $\mathcal{W}_2$ has the following form

$$\mathcal{W}_2 = \begin{pmatrix} S & \mathbf{0} \\ \mathbf{0} & \mathbf{1} \end{pmatrix} = \begin{pmatrix} 1 - \frac{1}{2} X X^\dagger & X & 0 \\ -X^\dagger & 1 - \frac{1}{2} X^\dagger X & 0 \\ 0 & 0 & 1 \end{pmatrix} \tag{A.20}$$

A.2 Complete diagonalization and physical neutrino masses

The block diagonal matrices m_ν, $m_\mathcal{S}$ and $m_\mathcal{N}$ can further be diagonalized to give physical masses for all neutral leptons by a unitary matrix $\mathcal{U}$ as

$$\mathcal{U} = \begin{pmatrix} U_\nu & 0 & 0 \\ 0 & U_S & 0 \\ 0 & 0 & U_N \end{pmatrix} . \tag{A.21}$$

where the unitary matrices U_ν, U_S and U_N satisfy

$$\begin{aligned} U_\nu^\dagger \, m_\nu \, U_\nu^* &= \hat{m}_\nu = \mathrm{diag}\left(m_{\nu_1}, m_{\nu_2}, m_{\nu_3}\right) \,, \\ U_S^\dagger \, m_\mathcal{S} \, U_S^* &= \hat{m}_S = \mathrm{diag}\left(m_{S_1}, m_{S_2}, m_{S_3}\right) \,, \\ U_N^\dagger \, m_\mathcal{N} \, U_N^* &= \hat{m}_N = \mathrm{diag}\left(m_{N_1}, m_{N_2}, m_{N_3}\right) \end{aligned} \tag{A.22}$$

With this discussion, the complete mixing matrix is

$$\begin{aligned} \mathcal{V} &= \mathcal{W} \cdot \mathcal{U} = \mathcal{W}_1 \cdot \mathcal{W}_2 \cdot \mathcal{U} \\ &= \begin{pmatrix} 1 - \frac{1}{2} Z Z^\dagger & -\frac{1}{2} Z Y^\dagger & Z \\ -\frac{1}{2} Y Z^\dagger & 1 - \frac{1}{2} Y Y^\dagger & Y \\ -Z^\dagger & -Y^\dagger & 1 - \frac{1}{2}(Z^\dagger Z + Y^\dagger Y) \end{pmatrix} \begin{pmatrix} 1 - \frac{1}{2} X X^\dagger & X & 0 \\ -X^\dagger & 1 - \frac{1}{2} X^\dagger X & 0 \\ 0 & 0 & 1 \end{pmatrix} \begin{pmatrix} U_\nu & 0 & 0 \\ 0 & U_S & 0 \\ 0 & 0 & U_N \end{pmatrix} \\ &= \begin{pmatrix} 1 - \frac{1}{2} X X^\dagger & X - \frac{1}{2} Z Y^\dagger & Z \\ -X^\dagger & 1 - \frac{1}{2}(X^\dagger X + Y Y^\dagger) & Y - \frac{1}{2} X^\dagger Z \\ 0 & -Y^\dagger & 1 - \frac{1}{2} Y^\dagger Y \end{pmatrix} \cdot \begin{pmatrix} U_\nu & 0 & 0 \\ 0 & U_S & 0 \\ 0 & 0 & U_N \end{pmatrix} \end{aligned} \tag{A.23}$$

B. One- and two-loop beta function coefficients for RG evolution of gauge couplings

Symmetry	$\boldsymbol{b_i}$	$\boldsymbol{b_{ij}}$
$G_{1_Y 2_L 3_C}$	$\begin{pmatrix} 41/10 \\ -19/6 \\ -7 \end{pmatrix}$	$\begin{pmatrix} 199/50 & 27/10 & 44/5 \\ 9/10 & 35/6 & 12 \\ 11/10 & 9/2 & -26 \end{pmatrix}$
$G_{1_{B-L} 1_Y 2_L 3_C}$	$\begin{pmatrix} 37/8 \\ 59/12 \\ -3 \\ -7 \end{pmatrix}$	$\begin{pmatrix} 209/16 & 63/8 & 9/4 & 4 \\ 63/8 & 33/4 & 3 & 12 \\ 3/2 & 1 & 8 & 12 \\ 1/2 & 3/2 & 9/2 & -26 \end{pmatrix}$
$G_{1_{B-L} 2_L 2_R 3_C}$	$\begin{pmatrix} 23/4 \\ -17/6 \\ -10/6 \\ -7 \end{pmatrix}$	$\begin{pmatrix} 253/8 & 9/2 & 171/4 & 4 \\ 3/2 & 37/3 & 6 & 12 \\ 57/4 & 6 & 93/2 & 12 \\ 1/2 & 9/2 & 9/2 & -26 \end{pmatrix}$
$G_{2_L 2_R 4_C}$	$\begin{pmatrix} -17/6 \\ 19/2 \\ -14/3 \end{pmatrix}$	$\begin{pmatrix} 37/3 & 6 & 45/2 \\ 6 & 1043/3 & 1275/2 \\ 9/2 & 255/2 & 800/2 \end{pmatrix}$
$G_{2_L 2_R 4_C D}$	$\begin{pmatrix} 19/2 \\ 19/2 \\ 2/3 \end{pmatrix}$	$\begin{pmatrix} 1043/3 & 6 & 1275/2 \\ 6 & 1043/3 & 1275/2 \\ 255/2 & 255/2 & 605 \end{pmatrix}$

Table 11: One and two loop beta coefficients for different gauge coupling evolutions described in text taking the second Higgs doublet at 1 TeV.

ACKNOWLEDGEMENT
Ram Lal Awasthi acknowledges the hospitality at Center of Excellence in Theoretical and Mathematical Sciences, SOA University where the present work has been completed.

References

[1] T. D. Lee and C. N. Yang, Phys. Rev. **D 104** (1956) 254.

[2] R. Foot, R.R. Volkas, Phys. Rev. D 52, 6595 (1995). Z.G. Berezhiani, R.N. Mohapatra, Phys. Rev. D 52, 6607 (1995).

[3] J. C. Pati and A. Salam, Phys. Rev. **D 8**, 1240 (1973); ibid. **D 10**, 275 (1974).

[4] R. N. Mohapatra and J. C. Pati, Phys. Rev. D **11**, 2558 (1975); Phys. Rev. D **11**, 566 (1975); G. Senjanovic and R. N. Mohapatra, Phys. Rev. D **12**, 1502 (1975).

[5] H. Georgi, Particles and Fields, *Proceedings of APS Division of Particles and Fields,* ed C. Carlson, (AIP, New York, 1975), p.575; H. Fritzsch, P. Minkowski, Ann. Phys. (Berlin) **93**, 193 (1975).

[6] P. Minkowski, *Phys. Lett.* **B 67**, 421 (1977); T. Yanagida in *Workshop on Unified Theories, KEK Report 79-18*, p. 95, 1979; M. Gell-Mann, P. Ramond and R. Slansky, *Supergravity*, p. 315. Amsterdam: North Holland, 1979; S. L. Glashow, *1979 Cargese Summer Institute on Quarks and Leptons*, p. 687, New York: Plenum, 1980;

R. N. Mohapatra and G. Senjanovic, Phys. Rev. Lett. **44**, 912 (1980).

[7] J. Schechter and J. W. F. Valle, Phys. Rev. **D 22**, 2227 (1980).

[8] M. Magg and C. Wetterich, Phys. Lett. **B 94**, 61 (1980); G. Lazaridis, Q. Shafi and C. Wetterich, Nucl. Phys. **B 181**, 287 (1981);

[9] R. N. Mohapatra and G. Senjanovic, Phys. Rev. **D 23**, 165 (1981).

[10] H. V. Klapdor-Kleingrothaus, A. Dietz, L. Baudis, G. Heusser, I. V. Krivosheina, S. Kolb, B. Majorovits, H. Pas et al., Eur. Phys. J. A12 (2001) 147-154; C. Arnaboldi et al. [CUORICINO Collaboration], Phys. Rev. C78, 035502 (2008); C. E. Aalseth et al. [IGEX Collaboration], Phys. Rev. D65 (2002) 092007; J. Argyriades et al. [NEMO Collaboration], Phys. Rev. **C 80**, 032501 (2009); I. Abt, M. F. Altmann, A. Bakalyarov, I. Barabanov, C. Bauer, E. Bellotti, S. T. Belyaev, L. B. Bezrukov et al., [hep-ex/0404039]; S. Schonert et al. [GERDA Collaboration], Nucl. Phys. Proc. Suppl. 145, 242-245 (2005); C. Arnaboldi et al. [CUORE Collaboration], Nucl. Instrum. Meth. A518, 775-798 (2004); H. V. Klapdor-Kleingrothaus, I. V. Krivosheina, A. Dietz, O. Chkvorets, Phys. Lett. B586, 198-212 (2004); H. V. Klapdor-Kleingrothaus, I. V. Krivosheina, Mod. Phys. Lett. A21, 1547-1566 (2006).

[11] H. V. Klapdor-Kleingrothaus, A. Dietz, L. Baudis, G. Heusser, I. V. Krivosheina, S. Kolb, B. Majorovits, H. Pas *et al.*, Eur. Phys. J. **A 12** (2001) 147-154; C. Aalseth *et al.*, Phys. Rev. **D 65**, 092007 (2002); H. V. Klapdor-Kleingrothaus *et al.*, Mod. Phys. Lett. **A 16**, 2409 (2001); H. V. Klapdor-Kleingrothaus, A. Dietz, and I.V. Krivosheina, Foundations of Physics **32**, 1181 (2002).

[12] E. Majorana, N. Cim. **14** (1937) 171.

[13] K. Abe *et al.*, [T2K collaboration], Phys. Rev. Lett. **107**, 041801 (2011); F. P. An *et al.*[DAYA-BAY Collaboration], Phys. Rev. Lett. **108**, 171803 (2012); P. Adamson *et al.*, [MINOS Collaboration], Phys. Rev. Lett. **107**, 181802 (2011); J. K. Ahn *et al.* [RENO Collaboration], Phys. Rev. Lett. **108**, 191802 (2012).

[14] V. Tello, M. Nemevšek, F. Nesti, G. Senjanović, F. Vissani, Phys. Rev. Lett. **106**, 151801 (2011); Joydeep Chakrabortty, H.Zeen Devi, Srubabati Goswami and Sudhanwa Patra, JHEP 1208 (2012) 008. arXiv:1204.2527 [hep-ph].

[15] M. Nemevsek, G. Senjanovic and V. Tello, arXiv: 1211.2837 [hep-ph].

[16] James Barry, Luis Dorame and Werner Rodejohann; Eur.Phys.J. C72 (2012) 2023, arXiv:1203.3365 [hep-ph].

[17] D. Chang, R. N. Mohapatra and M. K. Parida, Phys. Rev. Lett. **52**, 1072 (1984); D. Chang, R. N. Mohapatra and M. K. Parida, Phys. Rev. **D 30**, 1052 (1984).

[18] S. K. Kang and C. S. Kim, Phys. Lett. **B 646**, 248 (2007); J. Ellis, D. V. Nanopoulos and K. Olive, Phys. Lett. **B 300**, 121 (1993).

[19] S. K. Majee, M. K. Parida, and A. Raychaudhuri, Phys. Lett. **668**, 299 (2008); M. K. Parida and A. Raychaudhuri, Phys. Rev. **D 82**, 093017 (2010); S. K. Majee, M. K. Parida, A. Raychaudhuri, and U. Sarkar, Phys. Rev. **D 75**, 075003 (2007).

[20] G. Beall, M. Bander, and A. Soni, Phys Rev. Lett. 48 (1982) 848; A. Maiezza, M. Nemevsek, F. Nesti, and G. Senjanovic, Phys. Rev. **D 82**, 055022 (2010), arXiv: 1005.5160 [hep-ph]; D. Guadagnoli and R. N. Mohapatra, Phys.Lett. **B 694**, 386 (2011), arXiv: 1008.1074 [hep-ph]; S. Bertolini, J. O. Eeg, A. Maiezza and F. Nesti, Phys. Rev. **D 86** 095013 (2012), arXiv:1206.0668 [hep-ph].

[21] W. -Y. Keung and G. Senjanovic, Phys. Rev. Lett. **50**, 1427 (1983).

[22] Baldo-Ceolin, M. et al. Z.Phys. **C 63** (1994) 409-416 DFPD-94-EP-13.

[23] K. Arisaka et al. Phys.Rev.Lett. 70 (1993) 1049-1052.

[24] M.K. Parida and Sudhanwa Patra; Phys. Lett. **B 718** (2013) 1407.

[25] R. N. Mohapatra, Phys. Rev. Lett. **56**, 561-563 (1986); R. N. Mohapatra, J. W. F. Valle, Phys. Rev. **D34**, 1642 (1986).

[26] D. Wyler, L. Wolfenstein, Nucl. Phys. **B218**, 205 (1983); E. Witten, Nucl. Phys. **B268**, 79 (1986).

[27] W. Grimus and L. Lavoura, JHEP **0011**, 042 (2000), arXiv: 0008179 [hep-ph]; M. Hirsch, H. V. Klapdor-Kleingrothaus and O. Panella, Phys. Lett. B **374**, 7 (1996), arXiv: 9602306 [hep-ph]; M. Mitra, G. Senjanovic and F. Vissani, Nucl. Phys. B **856**, 26 (2012).

[28] K. Nakamura *et al.* (Particle Data Group), J. Phys.**G 37**, 075021 (2010); C. Amsler *et al.* (Particle Data Group), Phys. Lett. **B 667**, 1 (2008).

[29] C. R. Das and M. K. Parida, Eur. Phy. J. **C 20**, 121 (2001).

[30] P. S. B. Dev, R. N. Mohapatra, Phys. Rev. **D81**, 013001 (2010), [arXiv:0910.3924 [hep-ph]].

[31] Ram Lal Awasthi and Mina K. Parida, Phys.Rev. **D 86** (2012) 093004. e-Print: arXiv:1112.1826 [hep-ph].

[32] E. Akhmedov, M. Lindner, E. Schnapka, and J. W. F. Valle, Phys. Rev. **D 53**, 2752 (1996); arxiv:hep-ph/9509255.

[33] S. Antusch, J. P. Baumann, and E. Fernandez-Martinez, Nucl. Phys. **B 810**, 369 (2009); S. Antusch, M. Blennow, E. Fernandez-Martinez,and J. Lopez-Pavon, Phys. Rev. **D 80**, 033002 (2009); S. Antush, C. Biggio, E. Fernandez-Martinez, M. Belen Gavela, and J. Lopez-Pavon, J. High Energy Phys. **10** (2006) 084; D.V. Forero, S. Morisi, M. Tartola and J. W. F. Valle, J. High Energy Phys. **09** (2011) 142.

[34] E. Fernandez-Martinez, M. B. Gavela, J. Lopez-Pavon and O. Yasuda, Phys. Lett. **B 649**, 427 (2007); K. Kanaya, Prog. Theor. Phys.,**64**,2278 (1980); J. Kersten and A. Y. Smirnov, Phys. Rev. **D 76**, 073005 (2007); M. Malinsky, T. Ohlsson, H. Zhang, Phys. Rev. **D 79**, 073009 (2009); G. Altarelli and D. Meloni, Nucl. Phys. **B 809**, 158 (2009); F. del Aguila and J. A. Aguilar-Saavedra, Phys. Lett. **B 672**, 158 (2009); F. del Aguila and J. A. Aguilar-Saavedra and J. de Blas, Acta Phys. Polon. **B 40**, 2901 (2009); arXiv:0910.2720 [hep-ph]; A. van der Schaaf, J. Phys. **G 29**, 2755 (2003); Y. Kuno, Nucl. Phys. **B**, Proc. Suppl. **149**, 376 (2005).

[35] G. L. Fogli, E. Lisi, A. Marrone, A. Palazzo and A. M. Rotunno, Phys. Rev. D **84**, 053007 (2011), arXiv:1106.6028 [hep-ph]; T. Schwetz, M. Tartola and J. W. F. Valle, New J. Phys. **13**, 063004 (2011); D. V. Forero, M. Tartola and J. W. F. Valle,arXiv:1205.4018[hep-ph].

[36] R.N. Mohapatra; Phys. Rev. D 34 (1986) 909; M. Doi and T. Kotani, Prog. Theor. Phys. 89 (1993) 139; K. Muto, I. Blender, and H. V. Klapdor-Kleingrothaus, Z. Phys. **A 334** (1989) 177; M. Hirsch, K. Muto, T. Oda, and H. V. Klapdor-Kleingrothaus, Z. Phys. **A 347** (1994) 151; J.J. Gomez-Cadenas, J. Martin-Albo, M. Mezzetto, F. Monrabal, and M. Sorel, Riv.Nuovo Cim. 35 (2012) 29-98, e-Print: arXiv:1109.5515 [hep-ex]; J. Lopez-Pavon, S. Pascoli and Chan-fai Wong, arXiv:1209.5342 [hep-ph].

[37] A. Ilakovac, A. Pilaftsis, Nucl. Phys. **B437**, 491 (1995) [hep-ph/9403398]; F. Deppisch, J. W. F. Valle, Phys. Rev. **D72**, 036001 (2005) [hep-ph/0406040]; C. Arina, F. Bazzocchi, N. Fornengo, J. C. Romao, J. W. F. Valle, Phys. Rev. Lett. **101**, 161802 (2008) [arXiv:0806.3225 [hep-ph]]; M. Malinsky, T. Ohlsson, Z. -z. Xing, H. Zhang, Phys. Lett. **B 679**, 242-248 (2009) [arXiv:0905.2889 [hep-ph]]; M. Hirsch, T. Kernreiter, J. C. Romao, A. Villanova del Moral, JHEP **1001**, 103 (2010) [arXiv:0910.2435 [hep-ph]]; F. Deppisch, T. S. Kosmas, J. W. F. Valle, Nucl. Phys. **B 752**, 80-92 (2006) [arXiv:0910.3924 [hep-ph]].

[38] M. L. Brooks et al. [MEGA Collaboration], Phys. Rev. Lett. 83, 1521 (1999); B. Aubert [The BABAR Collaboration], arXiv:0908.2381 [hep-ex]; Y. Kuno (PRIME Working Group), Nucl. Phys. B. Proc. Suppl. 149, 376 (2005). For a review see F. R. Joaquim, A. Rossi, Nucl. Phys. B 765, 71 (2007).

[39] T. G. Rizzo, and G. Senjanovic, Phys.Rev. **D 25** 235 (1982); Phys.Rev. Lett. **46**, 1315 (1981); M. K. Parida and A. Raychaudhuri, Phys. Rev. **D 26**, 2364 (1982); M. K. Parida and C. C. Hazra, Phys. Lett. **B 121**, 355 (1983); M. K. Parida and C. C. Hazra, Phys. Rev. **D 40**, 3074 (1989).

[40] S. Bertolini, L. Di Luzio and M. Malinsky, Phys. Rev. **D 80**, 015013 (2009); S. Bertolini, L. Di Luzio and M. Malinsky, Phys. Rev. **D 85**, 095014 (2012); N. G. Deshpande, E. Keith, and P. Pal, Phys. Rev. **D 46**, 2261 (1992); D. G. Lee, R. N. Mohapatra, M. K. Parida and M. Rani, Phys. Rev. **D 51**, 229 (1995).

[41] D. Chang, R. N. Mohapatra, J. Gipson, R. E. Marshak, and M. K. Parida, Phys. Rev. **D 81**, 1718 (1985).

[42] H. Georgi, H. R. Quinn, and S. Weinberg, Phys. Rev. Lett. **33**, 451 (1974); D. R. T. Jones, Phys. Rev. **D 25**, 581 (1982).

[43] R.N. Mohapatra and R.E. Marshak, Phys. Rev. Lett. 44, 1316 (1980); [erratum- ibid. 44, 1643 (1980)]. For a recent review see R.N. Mohapatra, J. Phys. **G 36**, 104006 (2009).

[44] H. Nishino *et al.*, Phys. Rev. Lett. 102, 141801 (2009); H. Nishino *et al.*, Phys. Rev. **D 85**, 112001 (2012).

[45] K.S. Babu, J.C. Pati, and P. Rastogi, Phys.Lett. **B 621** (2005) 160-170.

[46] M.K. Parida and P.K. Patra, Phys. Rev. Lett. 66, 858 (1991); Phys. Rev. Lett. 68, 754 (1992).